Zeitschrift: Helvetica Physica Acta
Band: 42 (1969)
Heft: 7-8

Artikel: Metallic hydrogen. I
Autor: Schneider, T.
DOI: https://doi.org/10.5169/seals-114103

Metallic Hydrogen I[1])

by **T. Schneider**[2])

Delegation für Ausbildung und Hochschulforschung am E.I.R., 5303 Würenlingen, Schweiz

(11. VI. 69)

Summary. In this report we consider metallic hydrogen as an array of protons embedded in a sea of electrons. This system will be described in terms of the adiabatic approximation. The electronic contribution to the potential energy of the lattice will be calculated by use of a modified Hartree-Fock method. Starting from free electrons the electron-proton interaction will be introduced as a perturbation in a self-consistent manner. On this basis we shall discuss the following properties: Lattice energy, lattice dynamics, lattice stability, effective proton-proton interaction, electron band structure and superconductivity. In addition, we shall discuss the phase transition between molecular and metallic modifications. Results will enable us to make quantitative statements about the relation between electronic structure, crystal stability and phonon zero point energy. They suggest that increasing pressure leads to a phase transition from the metallic solid state into the liquid state due to the phonon zero point energy. The results furthermore imply interesting astrophysical consequences and indicate that metallic hydrogen may be a high temperature superconductor.

1. Introduction

Solid hydrogen is molecular in its ordinary modification [1]. WIGNER and HUNTINGTON [2] suggested that this modification becomes unstable under heavy pressure and changes into the metallic phase. They used the Wigner-Seitz method to estimate the cohesive energy of metallic hydrogen as a function of the volume. The results of WIGNER and HUNTINGTON imply that the binding energy and the atomic radius of the metallic modification are considerably smaller than the same quantities in the normal molecular crystal. However, the smallness of the atomic volume in the metallic phase is not at all unexpected. The intramolecular distance is 0.74 Å whereas the minimum intermolecular distance turns out to be 3.1 Å. Consequently the localization of the electrons in the molecule is nearly complete. On the other hand a delocalization of electrons is required in the metallic binding. This situation is certainly the case if the two distances discussed above are comparable. For the crystal structure at normal pressure and zero temperature this equality of distances may be achieved with an atomic radius of 0.8 Å. This value is in good agreement with the calculations of Wigner and Huntington. Therefore, this may indicate some evidence of the existence of a metallic phase at high pressures.

Due to the lack of a unified theory of binding it appears to be impossible at the time to describe this transition by means of a *single* energy-volume function. In

[1]) A summary of this paper was presented at the meeting of the Swiss Physical Society, at Berne, May 1969.

[2]) Now at IBM Zürich Research Lab., 8803 Rüschlikon, Switzeland.

certain cases this difficulty can be disentangled in virtue of a proposal due to KRONIG et al. [3]. In this model one discusses the volume dependence of the lattice energy of the molecular and the metallic modification. Figure 1 shows a schematic energy diagram and the corresponding pressure diagram. At low pressure and large volume the molecular phase is energetically in favour, while at high pressure and small volume this is the case for the metallic phase. At equilibrium pressure p_T there is an abrupt change in volume with a resulting destruction of the directional character of diatomic bonds. The two curves of the energy diagram have a common tangent at the volumes V_1 and V_2. Therefore, one hopes that an accurate calculation of the energy curve around the crossing point can be avoided.

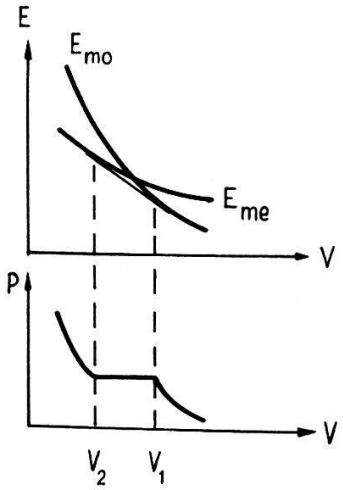

Figure 1

Schematic representation of energy and pressure diagrams for the molecular and metallic modifications, as suggested by KRONIG et al. [3].

In this treatment no account is taken of a possible layer structure with metallic binding within the layers and Van der Waals binding between them. It may be, of course, that this phase has a greater cohesive energy between V_1 and V_2 than the metallic and molecular modifications. However, this case is not considered here.

The problem is now to calculate the energy diagram of the metallic and the molecular phase. Such calculations were carried out by several authors. The values of the pressure of equilibrium are given by: KRONIG et al. [3], 0.7 Mbar; DAVYDOV [4], 1.85 Mbar; ABRIKOSOV [5], 2.4 Mbar; RAICH [6], 2 Mbar; TRUBITSYN [7], 4.6 Mbar.

The motivation of these investigations was a suggestion according to which the planets and especially Jupiter consist largely of hydrogen [8], [9]. It is quite clear that the appropriate equation of state is necessary in order to understand the structure of the planets.

Apart from these astrophysical consequences, one should keep in mind the fact that metallic hydrogen is one of the most simple systems. In ordinary metals the electron-ion interaction is weak, however, it appears to be very complicated. On the other hand the metallic hydrogen is characterized by a strong and quite simple electron-proton interaction. Owing to this fact and the considerably different masses of protons and ions one may expect additional interesting properties such as: pro-

nounced Kohn-anomalies, Friedel-oszillations and bandstructure effects; destruction of the lattice due to the phonon zero point energy and high-temperature superconductivity.

In the present paper we shall be concerned mainly with the properties of the metallic phase. The description of the molecular crystal will be taken from TRUBITSYN [7], [10]. Two terms, an electron exchange and a shielded Van der Waals term, are important for the intermolecular interaction. At present, this assumption leads to the most reliable information although its use at high pressure with resulting small inter molecular distances appears to be questionable.

The description of the metallic phase, on the other hand, is subject to less uncertainty. Metallic hydrogen will be considered here as an array of protons treated as point charges embedded in the sea of conduction electrons. In order to describe this system we shall start from the adiabatic and harmonic approximation. The electronic contribution to the lattice energy will be calculated using a modified Hartree-Fock method. Starting from free electrons we introduce the electron-proton interaction as a perturbation in a self-consistent manner. The electron correlation due to Coulomb interactions, however, will be treated approximately. This procedure enables a quantitative discussion of several properties of simple metals, especially of crystal stability, which as far as it concerns hydrogen was not investigated in previous works [2], [3], [5]–[7], [11]–[13]. The pure electron-ion interaction in these metals can be represented by a pseudo-potential while in metallic hydrogen it is given by a pure Coulomb interaction. A precise knowledge of these interactions enables us to avoid the difficulties usually associated with the pseudo-potential formalism.

In the second section we shall develop the basic theoretical formalism. The next four sections discuss the lattice energy, the lattice dynamics, and the effective proton-proton interaction in metallic hydrogen as well as the phase transition from the molecular into the metallic modification. Furthermore, we consider the lattice stability, the electronic properties of the metallic phase, and the possibility of superconductivity.

2. General Theory

In the discussion to follow we shall regard metallic hydrogen as an array of protons embedded in a sea of electrons. The Hamiltonian of this system is a sum of kinetic energies of electrons (T_e) and protons (T_I) and of the interactions between them.

$$
\begin{aligned}
H &= T_I + T_e + V_{ee} + V_{Ie}(\boldsymbol{R}) + V_{II}(\boldsymbol{R}) \,, \\
V_{ee} &= \frac{1}{2} \sum_i \sum_j{}' \frac{e^2}{r_{ij}} \,, \qquad V_{II}(\boldsymbol{R}) = \frac{1}{2} \sum_l \sum_{l'}{}' \frac{e^2}{|\boldsymbol{R}^l - \boldsymbol{R}^{l'}|} \\
V_{Ie} &= -\sum_i \sum_l \frac{e^2}{|\boldsymbol{r}_i - \boldsymbol{R}^l|} \,, \quad r_{ij} = |\boldsymbol{r}_i - \boldsymbol{r}_j| \,.
\end{aligned} \tag{1}
$$

In equation (1) $\boldsymbol{r}_i$ and $\boldsymbol{R}^l$ are the position vectors of the i'th electron and the l'th proton, respectively. $\boldsymbol{R}$ will always refer to the array of protons. A rigorous solution of the corresponding Schrödinger equation,

$$
H \Psi_G = E_G \Psi_G \tag{2}
$$

hardly appears possible. In the approximate solution to be discussed use will be made of the large mass difference between protons and electrons, leading to very different motions. Hence, initially one neglects the proton motion and investigates the electrons in the instantaneous field of the protons or ions. In the adiabatic Born-Oppenheimer approximation [16], [17] one first treats the motion of electrons in the field of stationary protons.

$$H_e(\boldsymbol{r}, \boldsymbol{R})\, \varphi_n(\boldsymbol{r}, \boldsymbol{R}) = \varepsilon_n(\boldsymbol{R})\, \varphi_n(\boldsymbol{r}, \boldsymbol{R}) \,. \tag{3}$$

Eigenvalues and eigenfunctions now depend only parametrically on the proton configuration. The crystal eigenfunctions Ψ_G can be expanded in terms of electron eigenfunctions φ_n:

$$\Psi_G = \sum_n X_{Gn}(\boldsymbol{R})\, \varphi_n(\boldsymbol{r}, \boldsymbol{R}) \,. \tag{4}$$

Substituting this expansion into equation (2), multiplying by φ_n^* from the left and integrating over $\boldsymbol{r}$ leads to the following set of equations for the functions X_{Gn}:

$$[T_I + \Phi_n(\boldsymbol{R}) + B_{nn}(\boldsymbol{R})]\, X_{Gn}(\boldsymbol{R}) + \sum_{m \neq n} C_{nm}(\boldsymbol{R})\, X_{Gm}(\boldsymbol{R}) = E_G\, X_{Gn}(\boldsymbol{R}) \tag{5}$$

where

$$C_{nm} = A_{nm} + B_{nm} \,, \tag{6}$$

$$A_{nm} = -\frac{\hbar^2}{M} \sum_l \int \varphi_n^*\, \nabla_{\boldsymbol{R}^l}\, \varphi_m\, d^3r\, \nabla_{\boldsymbol{R}^l} \qquad B_{nm} = -\frac{\hbar^2}{2M} \sum_l \int \varphi_n^*\, \nabla_{\boldsymbol{R}^l}^2\, \varphi_m\, d^3r \,, \tag{7}$$

$$\Phi_n(R) = V_{II}(\boldsymbol{R}) + \varepsilon_n(\boldsymbol{R}) \,. \tag{8}$$

The so-called adiabatic lattice equation is obtained by neglecting B_{nn} and C_{nm}:

$$[T_I + \Phi_n(\boldsymbol{R})]\, X_{Gn}(\boldsymbol{R}) = E_{Gn}\, X_{Gn}(\boldsymbol{R}) \,. \tag{9}$$

The approximate solution of the problem described by equation (2) is then given by the product function

$$\Psi_{Gn} = \varphi_n(\boldsymbol{r}, \boldsymbol{R})\, X_{Gn}(\boldsymbol{R}) \tag{10}$$

which must be regarded as the zeroth approximation. The neglected terms (B_{nn}, C_{nm}) can subsequently be treated as a perturbation. In the present work we shall be concerned with Schrödinger's equation for the electrons, equation (3), and the adiabatic lattice equation (9). It will be assumed that electrons are in the ground state, i.e. $n = 0$.

Adding and subtracting some terms to $\Phi_0(R)$, equation (8), one obtains

$$\Phi_0(\boldsymbol{R}) = \Phi_e(\boldsymbol{R}) + \Phi_c(\boldsymbol{R}) \tag{11}$$

where

$$\Phi_{oe}(\boldsymbol{R}) = \varepsilon_0(\boldsymbol{R}) + n \int V_p(\boldsymbol{r})\, d^3r - \frac{n^2}{2} \iint \frac{e^2}{|\boldsymbol{r}-\boldsymbol{r}'|}\, d^3r\, d^3r' \,, \tag{12}$$

$$V_p(\boldsymbol{r}) = \sum_l \frac{e^2}{|\boldsymbol{r}-\boldsymbol{R}^l|} \,.$$

Here $\Phi_c(R)$ is the energy of the proton lattice embedded in a homogeneous background of negative charge. The expression for $\Phi_c(R)$ is

$$\Phi_c(\boldsymbol{R}) = \frac{1}{2} \sum_l {\sum_{l'}}' \frac{e^2}{|\boldsymbol{R}^l - \boldsymbol{R}^{l'}|} - n \sum_l \int \frac{e^2}{|\boldsymbol{r}-\boldsymbol{R}^l|}\, d^3r + \frac{n^2}{2} \iint \frac{e^2}{|\boldsymbol{r}-\boldsymbol{r}'|}\, d^3r\, d^3r' \tag{13}$$

where n is the average density of protons or electrons; $n = N/\Omega$. This separation of the potential energy of the lattice is essential for the quantitative treatment to follow. $\Phi_c(R)$ can now be calculated by means of FUCHS' [19] generalization of Ewald's method. The result is

$$\Phi_c(\boldsymbol{R}) = \frac{N}{2} e^2 \left\{ \sum_{l \neq 0} \left[\frac{G(\varepsilon R^l)}{R^l} \right] - \frac{2\varepsilon}{\sqrt{\pi}} + 4\pi n \sum_{\boldsymbol{Q} \neq 0}' \left[|F(\boldsymbol{Q})|^2 \frac{e^{-Q^2/4\varepsilon^2}}{Q^2} \right] - \frac{\pi n}{\varepsilon^2} \right\} \tag{14}$$

where

$$F(\boldsymbol{Q}) = \frac{1}{N} \sum_l e^{-i\boldsymbol{Q}\boldsymbol{R}^l} \qquad G(y) = \frac{2}{\sqrt{\pi}} \int_y^\infty e^{-x^2} dx \tag{15}$$

$F(\boldsymbol{Q})$ is the structure factor and $\boldsymbol{R}^l$ is the distance of a given proton from its l'th neighbour. ε is a parameter that must be chosen so that the two sums converge.

A modified Hartree-Fock method is used to calculate the ground state energy of electrons, $\varepsilon_0(R)$, given by equation (3). These modifications are intended to eliminate the difficulties inherent in the usual approach. In the Hartree-Fock model single-electron eigenfunctions are solutions of Fock's system of equations:

$$[T_1 + V(\boldsymbol{r}_1) + V_c(\boldsymbol{r}_1) + V_{ex}(\boldsymbol{r}_1)]\, \varphi_k(\boldsymbol{r}_1) = E_k\, \varphi_k(\boldsymbol{r}_1) \tag{16}$$

where

$$V(\boldsymbol{r}_1) = -\sum_l \frac{e^2}{|\boldsymbol{r}_1 - \boldsymbol{R}^l|} \tag{17}$$

$$V_c(\boldsymbol{r}_1) = \int \frac{e^2}{r_{12}} \varrho(\boldsymbol{r}_2)\, d^3r_2 \tag{18}$$

$$V_{ex}(\boldsymbol{r}_1)\, \varphi_k(\boldsymbol{r}_1) = -\int \frac{e^2}{r_{12}} \varrho(\boldsymbol{r}_2, \boldsymbol{r}_1)\, \varphi_k(\boldsymbol{r}_2)\, d^3r_2 \tag{19}$$

$$\varrho(\boldsymbol{r}_2) = 2 \sum_{\boldsymbol{k}' \leqslant \boldsymbol{k}_F} \varphi^*_{\boldsymbol{k}'}(\boldsymbol{r}_2)\, \varphi_{\boldsymbol{k}'}(\boldsymbol{r}_2) \tag{20}$$

$$\varrho(\boldsymbol{r}_2, \boldsymbol{r}_1) = \sum_{\boldsymbol{k}' \leqslant \boldsymbol{k}_F} \varphi^*_{\boldsymbol{k}'}(\boldsymbol{r}_2)\, \varphi_{\boldsymbol{k}'}(\boldsymbol{r}_1)\,. \tag{21}$$

Here T_1 is the kinetic energy operator, $V(\boldsymbol{r}_1)$ is the electron-proton potential, $V_c(\boldsymbol{r}_1)$ is the Coulomb potential, and $V_{ex}(\boldsymbol{r}_1)$ is the exchange operator. Furthermore, $\boldsymbol{r}_i$ is the position vector of the i'th electron, the wave vector $\boldsymbol{k}$ is the electron quantum number, and $\boldsymbol{k}_F$ is the Fermi wave vector. The Hartree-Fock ground state energy of the electrons is

$$\varepsilon_0^{HF}(\boldsymbol{R}) = \sum_{\boldsymbol{k} \leqslant \boldsymbol{k}_F} E_k - \frac{1}{2} \iint \frac{e^2}{r^{12}} \varrho(\boldsymbol{r}_1)\, \varrho(\boldsymbol{r}_2)\, d^3r_1\, d^3r_2 + \frac{1}{2} \iint \frac{e^2}{r^{12}} \varrho(\boldsymbol{r}_2, \boldsymbol{r}_1)\, \varrho(\boldsymbol{r}_1, \boldsymbol{r}_2)\, d^3r_1\, d^3r_2\,. \tag{22}$$

The sum of single-electron energies E_k in the Hartree-Fock approach is not equal to the total energy. This is due to the fact that Coulomb energy and exchange energy enter twice into the sum.

In order to solve Fock's system of equations (16) we shall begin with free electrons and introduce the electron-proton potential, the exchange potential, and the Coulomb potential as perturbations. In zeroth approximation we have

$$T\,|\boldsymbol{k}\rangle = E^0_{\boldsymbol{k}}\,|k\rangle \tag{23}$$

where

$$E_{\boldsymbol{k}}^0 = \frac{\hbar^2}{2\,m}\,k^2, \quad |k\rangle = \Omega^{-1/2}\,e^{i\boldsymbol{k}\boldsymbol{r}}\,. \tag{24}$$

The electron-proton potential, the change in single-electron eigenfunctions due to it, and the correspondingly modified Coulomb and exchange potentials will be treated as perturbations. In first approximation the electron eigenfunction becomes:

$$\varphi_{\boldsymbol{k}} = |k\rangle + |\boldsymbol{k}), \quad |\boldsymbol{k}) = \sum_{k' \neq k} b_{\boldsymbol{k}'\boldsymbol{k}}\,|\boldsymbol{k}'\rangle\,. \tag{25}$$

In order to determine the expansion coefficients $b_{\boldsymbol{k}'\boldsymbol{k}}$ and the energy $E_{\boldsymbol{k}}$ to second order, equation (25) is substituted into equation (16) and terms of equal order are equated to each other. This results in the following set of equations:

$$T_1\,|\boldsymbol{k}\rangle = E_{\boldsymbol{k}}^0\,|\boldsymbol{k}\rangle \tag{26}$$

$$T\,|\boldsymbol{k}) + W\,|\boldsymbol{k}\rangle = E_{\boldsymbol{k}}^0\,|\boldsymbol{k}) + E_{\boldsymbol{k}}^1\,|\boldsymbol{k}\rangle \tag{27}$$

$$W\,|\boldsymbol{k}) = E_{\boldsymbol{k}}^1\,|\boldsymbol{k}) + E_{\boldsymbol{k}}^2\,|\boldsymbol{k}\rangle \tag{28}$$

where

$$W(\boldsymbol{r}_1) = V_c^0(\boldsymbol{r}_1) + V_{ex}^0(\boldsymbol{r}_1) + U(\boldsymbol{r}_1) \tag{29}$$

$$U(\boldsymbol{r}_1) = V(\boldsymbol{r}_1) + V_c^1(\boldsymbol{r}_1) + V_{ex}^1(\boldsymbol{r}_1)\,. \tag{30}$$

Using equations (18)–(21) the individual terms become

$$V_c^0(\boldsymbol{r}_1) = \int \frac{e^2}{|\boldsymbol{r}_1-\boldsymbol{r}_2|}\,\varrho^0(\boldsymbol{r}_2)\,d^3r_2\,, \quad \varrho^0(\boldsymbol{r}_2) = 2\sum_{\boldsymbol{k}' \leqslant k_F} \langle \boldsymbol{k}'|\,|\boldsymbol{k}'\rangle$$

$$V_c^1(\boldsymbol{r}_1) = \int \frac{e^2}{|\boldsymbol{r}_1-\boldsymbol{r}_2|}\,\varrho^1(\boldsymbol{r}_2)\,d^3r_2\,, \quad \varrho^1(\boldsymbol{r}_2) = 2\sum_{\boldsymbol{k}' \leqslant k_F} \langle \boldsymbol{k}'|\,|\boldsymbol{k}') + (\boldsymbol{k}'|\,|\boldsymbol{k}'\rangle$$

$$V_{ex}^0(\boldsymbol{r}_1)\,f(\boldsymbol{r}_1) = -\int \frac{e^2}{|\boldsymbol{r}_1-\boldsymbol{r}_2|}\,\varrho^0(\boldsymbol{r}_1,\boldsymbol{r}_2)\,f(\boldsymbol{r}_2)\,d^3r_2\,, \quad \varrho^0(\boldsymbol{r}_1,\boldsymbol{r}_2) = \sum_{\boldsymbol{k}' \leqslant k_F} \langle \boldsymbol{k}'|\,|\boldsymbol{k}'\rangle$$

$$V_{ex}^1(\boldsymbol{r}_1)\,f(\boldsymbol{r}_1) = -\int \frac{e^2}{|\boldsymbol{r}_1-\boldsymbol{r}_2|}\,\varrho^1(\boldsymbol{r}_1,\boldsymbol{r}_2)\,f(\boldsymbol{r}_2)\,d^3r_2, \quad \varrho^1(\boldsymbol{r}_2,\boldsymbol{r}_1) = \sum_{\boldsymbol{k}' \leqslant k_F} \langle \boldsymbol{k}'|\,|\boldsymbol{k}') + (\boldsymbol{k}'|\,|\boldsymbol{k}'\rangle\,.$$

Multiplication of equation (27) by $\langle \boldsymbol{k}'|$ gives

$$b_{\boldsymbol{k}'\boldsymbol{k}} = \frac{\langle \boldsymbol{k}'|\,U\,|\boldsymbol{k}\rangle}{E_{\boldsymbol{k}}^0 - E_{\boldsymbol{k}'}^0}\,. \tag{31}$$

Multiplying equations (27) and (28) by $\langle k|$ and using equation (31) one obtains the following contributions to the energy in first and second order:

$$E_k^1 = \langle \boldsymbol{k}|\,V + V_c^0 + V_{ex}^0\,|\boldsymbol{k}\rangle \tag{32}$$

$$E_k^2 = \sum_{\boldsymbol{k}' \neq \boldsymbol{k}} b_{\boldsymbol{k}'\boldsymbol{k}}\,\langle \boldsymbol{k}|\,U\,|\boldsymbol{k}'\rangle = \sum_{\boldsymbol{k}' \neq \boldsymbol{k}} \frac{\langle \boldsymbol{k}'|\,U\,|\boldsymbol{k}\rangle\langle \boldsymbol{k}|\,U\,|\boldsymbol{k}'\rangle}{E_{\boldsymbol{k}}^0 - E_{\boldsymbol{k}}^0}\,. \tag{33}$$

In this perturbation calculation the approximate solution one is looking for (equation (25)) was substituted into the Coulomb and exchange potentials, equations (29) and (30). This generates a self-consistent potential U, equation (30), containing the

electron-proton potential and the change this produces in the Coulomb and exchange potentials. In the following, U will denote the self-consistent or shielded electron-proton interaction, while V will refer to the bare electron-proton interaction. Use of equations (30) and (31) results in the following relation between matrix elements of these potentials:

$$\langle \boldsymbol{k}+\boldsymbol{Q}\,|\,U\,|\,\boldsymbol{k}\rangle = \langle \boldsymbol{k}+\boldsymbol{Q}\,|\,V+V_c^1+V_{ex}^1\,|\,\boldsymbol{k}\rangle$$
$$= \langle \boldsymbol{k}+\boldsymbol{Q}\,|\,V\,|\,\boldsymbol{k}\rangle + 4\pi e^2 \frac{1}{\Omega}\sum_{k'\leqslant k_F} \frac{\langle \boldsymbol{k}'+\boldsymbol{Q}\,|\,U\,|\,\boldsymbol{k}'\rangle}{E^0_{\boldsymbol{k}'}-E^0_{\boldsymbol{k}'+\boldsymbol{Q}}}\left[\frac{4}{Q^2}-\frac{1}{|\boldsymbol{k}-\boldsymbol{k}'|^2}-\frac{1}{|\boldsymbol{k}-\boldsymbol{k}'-\boldsymbol{Q}|^2}\right]. \quad (34)$$

The first term in square brackets arises from the Coulomb potential $V_c(\boldsymbol{r}_1)$, while remaining terms come from the exchange potential $V^1_{ex}(\boldsymbol{r}_1)$. These exchange terms have poles of second order at $\boldsymbol{k}'=\boldsymbol{k}$ and $\boldsymbol{k}'=\boldsymbol{k}-\boldsymbol{Q}$. The singularities can be avoided if account is taken of electron correlations due to Coulomb interactions which are neglected in the Hartree-Fock method. The neglected effect describes the influence of electron correlations on the individual motion of electrons. It can be taken into account by shielding the exchange terms, resulting in the following expression,

$$\langle \boldsymbol{k}+\boldsymbol{Q}\,|\,U\,|\,\boldsymbol{k}\rangle = \langle \boldsymbol{k}+\boldsymbol{Q}\,|\,V\,|\,\boldsymbol{k}\rangle + \frac{4\pi e^2}{\Omega}\sum_{k'\leqslant k_F} \frac{\langle \boldsymbol{k}'+\boldsymbol{Q}\,|\,U\,|\,\boldsymbol{k}'\rangle}{E^0_{\boldsymbol{k}'}-E^0_{\boldsymbol{k}'+\boldsymbol{Q}}}\left[\frac{4}{Q^2}-\frac{1}{|\boldsymbol{k}-\boldsymbol{k}'|^2+k_s^2}-\frac{1}{|\boldsymbol{k}-\boldsymbol{k}'-\boldsymbol{Q}|^2+k_s^2}\right] \quad (35)$$

which replaces equation (34). Here k_s is the reciprocal shielding length.

The bare electron-proton potential occurring in this equation is of the same form as equation (17)

$$V(\boldsymbol{r}_1)=\sum_l V_I(|\boldsymbol{r}_1-\boldsymbol{R}^l|)=-\sum_l \frac{e^2}{|\boldsymbol{r}_1-\boldsymbol{R}^l|}.$$

Thus, matrix elements $\langle \boldsymbol{k}+\boldsymbol{Q}\,|\,V(\boldsymbol{r}_1)\,|\,\boldsymbol{k}\rangle$ can be factorized into a structure factor $F(\boldsymbol{Q})$ and a form factor $V_I(Q)$.

$$\langle \boldsymbol{k}+\boldsymbol{Q}\,|\,V(\boldsymbol{r}_1)\,|\,\boldsymbol{k}\rangle = F(\boldsymbol{Q})\,V_I(Q) \quad (36)$$

where

$$F(\boldsymbol{Q})=\frac{1}{N}\sum_l e^{-i\boldsymbol{Q}\boldsymbol{R}^l} \quad (37)$$

$$V_I(Q)=-\frac{4\pi n e^2}{Q^2}=\frac{N}{\Omega}\int e^{-i\boldsymbol{Q}\boldsymbol{x}}\,V_I(x)\,d^3x\,. \quad (38)$$

In the equations above, $F(\boldsymbol{Q})$ describes the proton array and $V_I(Q)$ is the Fourier transform of the bare electron-proton potential. An analogous factorization of matrix elements belonging to the self-consistent electron-proton potential seems possible only if one eliminates the dependence on $\boldsymbol{k}$ and $\boldsymbol{k}'$ of both exchange terms occurring in the determining equation. This dependence on $\boldsymbol{k}$ reflects the spatially non-local character of V^1_{ex}, equation (30). Following a suggestion by KLEINMAN [19] we shall eliminate this non-localness by use of the following averaging procedure:

$$|\boldsymbol{k}-\boldsymbol{k}'|^2+k_s^2 \to \langle|\boldsymbol{k}-\boldsymbol{k}'|^2\rangle+k_s^2=\frac{6}{5}k_F^2+k_s^2\approx k_F^2+k_s^2$$
$$|\boldsymbol{k}-\boldsymbol{k}'-\boldsymbol{Q}|^2+k_s^2 \to \langle|\boldsymbol{k}-\boldsymbol{k}'-\boldsymbol{Q}|^2\rangle+k_s^2=\frac{6}{5}k_F^2+Q^2+k_s^2\approx k_F^2+Q^2+k_s^2. \quad (39)$$

In this approximation exchange terms in the determining equation depend only on Q. Their Fourier transforms thus correspond to a purely local potential, i.e. one which depends on r only. Using equations (35), (36) and (38) the following simple linear relation is found to exist between the Fourier components of the self-consistent potential and the bare electron-proton potential:

$$U_I(Q) = \frac{V_I(Q)}{\varepsilon_e(Q)} \tag{40}$$

where

$$\langle \boldsymbol{k} + \boldsymbol{Q} \mid U \mid \boldsymbol{k} \rangle = F(\boldsymbol{Q})\, U_I(Q) \tag{41}$$

$$\varepsilon_e(Q) = 1 + \chi(Q)\,[1 - C(Q)] \tag{42}$$

$$\chi(Q) = \frac{4\pi n e^2}{Q^2} \frac{3}{2 E_F^0} f(Q/2 k_F), \qquad f(t) = \frac{1}{2} + \frac{1-t^2}{4t} \ln \left| \frac{1+t}{1-t} \right|$$

$$E_F^0 = \frac{\hbar^2}{2m} k_F^2, \qquad n = \frac{N}{\Omega}$$

$$C(Q) = \frac{1}{4} \left[\frac{Q^2}{p\, k_F^2} + \frac{Q^2}{p\, k_F^2 + Q^2} \right], \qquad p = 1 + \left(\frac{k_s}{k_F} \right)^2.$$

In these expressions $\varepsilon_e(Q)$ is the static dielectric function of the electron gas. The limiting values

$$\varepsilon_e(Q) = 1 + \lambda^2/Q^2, \quad \text{small } Q \qquad \varepsilon_e(Q) = 1 - \lambda^2/3\, p\, Q^2, \quad \text{large } Q \tag{43}$$

with

$$\lambda = \frac{k_F}{\pi a_0}$$

indicate that the electron gas has a strong shielding effect on Fourier coefficients with small Q and a weak shielding effect on those with large Q.

The approximate solution, equation (40), of equation (35) outlined above has been successfully applied in recent years to the quantitative analysis of simple metals [14], [15], [20]–[24]. In spite of this success it should not be overlooked that the inherent non-localness of the exchange terms has been neglected. In the treatment to follow we shall use the approximate solution given by equation (40). Based on this we can use equations (24), (32), (33) and (41) to compute the single-electron energy, while equations (12), (22) and (41) may be used to obtain the contribution of electrons to the potential energy of the lattice. In second order one has

$$E_{\boldsymbol{k}}^{HF} = \frac{\hbar^2}{2m} k^2 + \frac{6}{5} \frac{e^2}{r_s} - \frac{2 e^2}{\pi} k_F f\left(\frac{k}{k_F}\right) - \frac{3}{2} \frac{e^2}{r_s} + \sum_{\boldsymbol{Q} \neq 0} |F(\boldsymbol{Q})|^2 \frac{U_I^2(Q)}{E_{\boldsymbol{k}}^0 - E_{\boldsymbol{k}+\boldsymbol{Q}}^0} \tag{44}$$

$$\Phi_{oe}^{HF} = N \left[\frac{3}{5} E_F^0 - \frac{3 e^2}{4\pi} k_F + E_b \right] \tag{45}$$

with

$$E_b = -\frac{1}{2} \sum_{\boldsymbol{Q} \neq 0} |F(\boldsymbol{Q})|^2\, U_I(Q)\, V_I(Q)\, X(Q) \tag{46}$$

$$X(Q) = \frac{3}{2 E_F^0} f(Q/2 k_F) \qquad \frac{4\pi}{3} r_s^3 = \frac{\Omega}{N} = \frac{1}{n}.$$

The first term in the single electron energy is the energy of a free electron. The second term is the Coulomb energy, the third is the exchange energy, and the fourth is the mean value of the bare electron-proton potential. These three terms are contributions of first order. The last term is of second order and accounts for the effects of band structure. The electronic contribution to the potential energy of the lattice, equation (45), is the sum of the zero point energy of free electrons, the exchange energy, and a second order term depending on the proton configuration. The difference between this and the corresponding term in the single electron energy is due to the exchange Coulomb-interaction entering twice into the sum of single electron energies.

In the Hartree-Fock method outlined above electron correlation due to the Coulomb interaction is included in second order contributions only, i.e. in terms depending on $U_I(Q)$. Having started with free electrons the correlation energy to be considered next is of first order. According to NOZIÈRES and PINES [25] this correlation energy can be estimated to be

$$\frac{\varepsilon^{\text{corr}}}{N} = (0.678 \ln r_0 - 2.505)\, 10^{-12} \text{ erg} \tag{47}$$

where

$$r_0 = r_s/a_0$$

with a_0 being the Bohr radius. The total electronic contribution to the potential energy of the lattice per electron thus amounts to, cf. equations (45) and (47),

$$\Phi_{oe} = \Phi_{oe}^{HF} + \varepsilon^{\text{corr}} . \tag{48}$$

As is well known, the Hartree-Fock single electron energy, equation (44), leads to an unrealistic density of states on the Fermi sphere. This difficulty is due to the k-dependence of the exchange term and can be avoided by taking account of the electron correlation. In analogy to the defining equation (40) we shall use an approximation in which exchange and correlation potentials are approximated by local potentials. In this case exchange energy and correlation energy will depend on electron density only, the k-dependence having been replaced by an appropriate average. To derive an expression for these energies we shall start from the total correlation and exchange energies. Using equations (45) and (47) one finds

$$\varepsilon(N) = N\, \varepsilon^{ex}(N) + N\, \varepsilon^{\text{corr}}(N) \tag{49}$$

where

$$\varepsilon^{ex}(N) = -\frac{3\, e^2}{4\, \pi}\, k_F , \quad \varepsilon^{\text{corr}}(N) = (-2.505 + 0.678 \ln r_0)\, 10^{-12} \text{ erg}$$

$$k_F^3 = 3\, \pi^2\, N/\Omega , \qquad \frac{4\, \pi}{3}\, r_0^3 = \frac{\Omega}{a_0^3\, N} .$$

Next we add another electron to the N electrons already present. The energy now becomes $\varepsilon\ (N + 1)$. The energy difference

$$\mu = \varepsilon\ (N + 1) - \varepsilon(N) = \frac{\partial \varepsilon}{\partial N} \tag{50}$$

is known as the chemical potential arising from the exchange and correlation of electrons. It is the required exchange and correlation energy of an electron on the Fermi sphere. Using equations (49) and (50) one obtains

$$\mu = \mu^{ex} + \mu^{\text{corr}} \tag{51}$$

with

$$\mu^{ex} = -\frac{e^2}{\pi} k_F$$

$$\mu^{\text{corr}} = [0.678 \ln r_0 - 2.731]\, 10^{-12} \text{ erg} . \tag{52}$$

In accordance with the definition of μ^{ex} this expression agrees with the exchange energy, equation (44), of an electron on the Fermi sphere. The following single electron energy is obtained from equation (51), replacing equation (44):

$$E_{\boldsymbol{k}} = \frac{\hbar^2}{2m} k^2 - \frac{3}{10} \frac{e^2}{r_s} + \mu + \sum_{\boldsymbol{Q} \neq 0} |F(\boldsymbol{Q})|^2 \frac{U_I^2(Q)}{E^0_{\boldsymbol{k}} - E^0_{\boldsymbol{k}+\boldsymbol{Q}}} . \tag{53}$$

For a quantitative analysis of properties derivable from the single electron energy and the lattice energy it is necessary to determine the shielding length k_s appearing in the dielectric function of equation (43). Following GELDART and VOSKO [26] we shall make use of the fact that the compressibility of the electron gas can be derived either from the total energy, or from the dielectric response function. This dielectric function, according to NOZIÈRES and PINES [27], is defined by the relation

$$V_t(Q) = \frac{V_I(Q)}{\varepsilon_t(Q)} \tag{54}$$

where $V_t(Q)$ is the potential experienced by a proton when the system is subjected to an external perturbation $V_I(Q)$. $V_t(Q)$ consists of the external perturbation $V_I(Q)$ and the Coulomb interaction of the proton with the electron charge $-e\,\varrho_e(Q)$, i.e.

$$V_t(Q) = V_I(Q) - \frac{4\pi n e^2}{Q^2} \varrho_e(Q) . \tag{55}$$

Use of equations (38) and (46) shows that

$$U_I(Q)\, V_I(Q)\, X(Q) = -\frac{4\pi n e^2}{Q^2} U_I(Q)\, X(Q) = -\frac{4\pi n e^2}{Q^2} \varrho_e(Q) . \tag{56}$$

Compressibility and dielectric response function are related through the expression [23]

$$\lim_{Q \to 0} Q^2 \varepsilon(Q) = 4\pi n e^2 \varkappa . \tag{57}$$

Using equation (56) and the function defined in equation (42) we obtain

$$\frac{\varkappa}{\varkappa_0} = \frac{1}{1 - (2/\pi q_0 k_F p)} \tag{58}$$

with

$$\varkappa_0 = \frac{1}{n} \frac{3}{2 E_F^0} .$$

This expression can now be compared with the compressibility derived from the total energy of the unperturbed electron gas. The total energy is, cf. equations (45) and (48),

$$\frac{\varepsilon}{N} = \frac{3}{5} E_F^0 - \frac{3 e^2}{4\pi} k_F - (2.505 - 0.678 \ln r_0)\, 10^{-12} \text{ erg} .$$

Hence, using

$$\frac{1}{\varkappa} = \Omega \frac{\partial^2 \varepsilon}{\partial \Omega^2}$$

one obtains the following expression for the compressibility:

$$\frac{\varkappa}{\varkappa_0} = \frac{1}{1-(1/\pi\, a_0\, k_F) - (C_0\, a_0\, \pi^2/e^2(\pi\, a_0\, k_F)^2)} \tag{59}$$

with

$$C_0 = 0.678\ 10^{-12}\ \text{erg}\ .$$

Both expressions must agree with one another since both describe the compressibility of the electron gas. This enables us to determine p and k_s. Using equations (58) and (59) we find

$$p = \frac{2}{1+0.153\ (1/\pi\, a_0\, k_F)} = 1 + \left(\frac{k_s}{k_F}\right)^2. \tag{60}$$

These approximate expressions for the electron energy, equation (53), and the electronic contribution to the lattice energy, equation (48), permit a quantitative evaluation of the metallic hydrogen properties of interest. The following approximations were made in the derivation of these energies:

(a) adiabatic approximation,

(b) self-consistent second order perturbation calculation,

(c) elimination of the non-local character of the exchange potential.

An investigation into the validity of the adiabatic approximation is in progress. Regarding the perturbation calculation is should be pointed out that inclusion of third order effects would lead to three-body forces. We surmise that these three-body forces can be neglected. The crystal structure realized at absolute zero could be verified in several instances for simple metals on the basis of two-body forces [15], [20]–[22]. Finally, the choice of free electrons as a starting point for the perturbation calculation allows a self-consistent, simple, and quantitative description of the system. The non-local character of the exchange potential was, however, eliminated in this description. While this approximation has been used successfully to describe a number of simple metals, a numerical solution of the problem nevertheless would seem desirable in order to have a quantitative evaluation of the extent and consequences of the non-local character of the potential.

3. Lattice Energy, Lattice Dynamics and Effective Proton-Proton Interaction

At absolute zero the lattice energy of metallic hydrogen consists of the potential energy of the fixed lattice and of the phonon zero point energy, i.e.

$$E_G^{me} = \Phi_0(\mathring{\boldsymbol{R}}) + \frac{1}{2}\sum_{\boldsymbol{q},\,\alpha} \hbar\,\omega_\alpha(\boldsymbol{q})\ . \tag{61}$$

Here $\mathring{\boldsymbol{R}}$ characterizes the proton configuration in the fixed lattice, while $\omega_\alpha(\boldsymbol{q})$ denotes frequency of a phonon having wave vector $\boldsymbol{q}$ and belonging to branch α. With the aid of relations (11), (14), (45) and (48) we can derive the following expressions for the energy per electron of the fixed lattice:

$$\Phi_0(\mathring{\boldsymbol{R}}) = \Phi_{oe}(\mathring{\boldsymbol{R}}) + \Phi_c(\mathring{\boldsymbol{R}}) \tag{62}$$

where

$$\Phi_{oe}(\overset{\circ}{\boldsymbol{R}}) = \frac{3}{5} E_F^0 - \frac{3\,e^2}{4\,\pi} k_F + \frac{\varepsilon^{\mathrm{corr}}}{N} - \frac{1}{2} \sum_{\boldsymbol{h}\neq 0} |F(\boldsymbol{h})|^2 U_I(h)\, V_I(h)\, X(h) \tag{63}$$

$$\Phi_c(\overset{\circ}{\boldsymbol{R}}) = \frac{e^2}{2\,r_s}\,\alpha \tag{64}$$

$$\alpha = \sum_{l,\varkappa\varkappa'} \frac{1}{\sigma} \left[\frac{G[X\binom{l\,0}{\varkappa\varkappa'}]}{X\binom{l\,0}{\varkappa\varkappa'}}\right] - \frac{2}{\sqrt{\pi}} + 3\left[|F(\boldsymbol{h}')|^2 \frac{e^{-h'^2/4}}{h'^2} - \frac{1}{4}|F(0)|^2\right]$$

$$\boldsymbol{h}' = \boldsymbol{h}\, r_s\,, \quad \boldsymbol{X}\binom{l\,l'}{\varkappa\varkappa'} = \frac{1}{r_s}\left[\overset{\circ}{\boldsymbol{R}}\binom{l}{\varkappa} - \overset{\circ}{\boldsymbol{R}}\binom{l'}{\varkappa'}\right], \quad \varepsilon = 1/r_s\,.$$

In these equations $\boldsymbol{h}$ is a reciprocal lattice vector, $\overset{\circ}{\boldsymbol{R}}\binom{l}{\varkappa}$ is a vector denoting the equilibrium position of the $\varkappa$'th atom in the l'th elementary cell and σ is the number of atoms in that cell. The purely volume dependent terms in the potential energy of the lattice are collected together by applying the following transformation:

$$\Phi_0(\overset{\circ}{\boldsymbol{R}}) = \Phi(\Omega) + \Phi^s_{oe}(\overset{\circ}{\boldsymbol{R}}) + \Phi^s_c(\overset{\circ}{\boldsymbol{R}}) \tag{65}$$

where

$$\Phi_0(\Omega) = \frac{3}{5} E_F^0 - \frac{3\,e^2}{4\,\pi} k_F - \frac{9}{10}\frac{e^2}{r_s} + \frac{\varepsilon^{\mathrm{corr}}}{N}$$

$$\Phi^s_c(\overset{\circ}{\boldsymbol{R}}) = -\frac{1}{2} \sum_{\boldsymbol{h}\neq 0} |F(\boldsymbol{h})|^2 U_I(h)\, V_I(h)\, X(h) = \frac{1}{2} \sum_{\boldsymbol{h}\neq 0} |F(\boldsymbol{h})|^2 U_e(h)$$

$$\Phi^s_c(\overset{\circ}{\boldsymbol{R}}) = \frac{e^2}{r_s}\left[\frac{\alpha}{2} + \frac{9}{10}\right]$$

$\Phi_0(\Omega)$ is the energy per electron of electrons homogeneously distributed in a Wigner-Seitz sphere, and depends only on volume. The second order contribution to this energy, Φ^s_{oe}, and the electrostatic term Φ^s_c depend on volume and crystal structure. The structure dependence of the electrostatic term is expressed by the α-coefficient. Numerical values of α for the bcc, fcc and hcp lattices are listed in Table I. In hcp-lattices α will, of course, depend on the axis ration c/a. It is remarkable that α, and hence Φ^s_c, acquire their minimum values for the ideal axis ratio (Fig. 2), and that the bcc-lattice, among the lattices considered, leads to the lowest electrostatic energy. In addition to the electrostatic energy, Φ^s_{oe} and the zero-point energy of equation (61) are also dependent on crystal structure.

Table I

Numerical values of α for bcc-, fcc- and hcp-crystal structures. c/a is the axis ratio.

	c/a	$-\alpha$	c/a	$-\alpha$
bcc	–	1.79186	1.6	1.7916
fcc	–	1.79172	$\sqrt{8/3}$	1.7917
hcp	1.2	1.7755	1.7	1.7913
	1.3	1.7817	1.8	1.7891
	1.4	1.7866	1.9	1.7850
	1.5	1.7900	2	1.7789

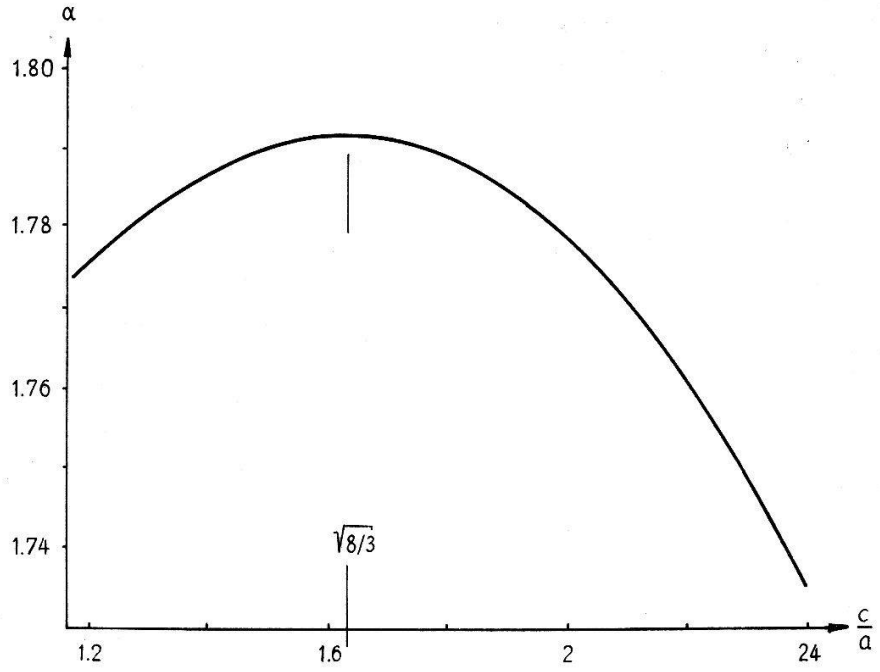

Figure 2

Dependence of coefficient α on axis ratio c/a in the hcp-lattice.

The harmonic approximation is used for calculating the zero point energy. The Hamiltonian of the lattice oscillations can be written

$$H = T_I + \frac{1}{2} \sum_{\substack{l,\varkappa,i \\ l',\varkappa',j}} \Phi_{ij} \begin{pmatrix} l\, l' \\ \varkappa\, \varkappa' \end{pmatrix} u_i \begin{pmatrix} l \\ \varkappa \end{pmatrix} u_j \begin{pmatrix} l' \\ \varkappa' \end{pmatrix} \tag{66}$$

where

$$\Phi_{ij} \begin{pmatrix} l\, l' \\ \varkappa\, \varkappa' \end{pmatrix} = \frac{\partial^2 \Phi}{\partial u_i \begin{pmatrix} l \\ \varkappa \end{pmatrix} \partial u_j \begin{pmatrix} l' \\ \varkappa' \end{pmatrix}} \Bigg|_{\substack{\text{all} \\ u_i \begin{pmatrix} l \\ \varkappa \end{pmatrix} = 0}} \tag{67}$$

$$\Phi_0 = \Phi_0(\Omega) + \Phi_{oe}(\boldsymbol{R}) + \Phi_c(\boldsymbol{R})$$

and Φ_0 is the potential energy of the proton lattice, equations (11), (14) and (48). $u_i \begin{pmatrix} l \\ \varkappa \end{pmatrix}$ is the i'th component of the displacement from equilibrium of the n'th atom in the $\varkappa$'th cell. With the aid of equation (67) and the equations of motion one obtains the dynamic equations (68) in the usual manner. They allow us to determine the normal frequencies and the polarization vector $\boldsymbol{e}(\varkappa, \boldsymbol{q})$ where $\boldsymbol{q}$ is the wave vector of the lattice vibration.

$$\sum_{\varkappa',j} [D_{ij}^{\varkappa\varkappa'}(\boldsymbol{q}) - \delta_{ij}\, \delta_{\varkappa\varkappa'}\, M\, \omega^2(\boldsymbol{q})]\, e_j(\varkappa', \boldsymbol{q}) = 0 \quad (i, j) = 1, 2, 3\,, \quad \varkappa = 1 \ldots \delta \tag{68}$$

with

$$D_{ij}^{\varkappa\varkappa'}(\boldsymbol{q}) = \sum_l \Phi_{ij} \begin{pmatrix} 0\, l \\ \varkappa\, \varkappa' \end{pmatrix} e^{-i\boldsymbol{q}\left[\mathring{\boldsymbol{R}}\begin{pmatrix} 0 \\ \varkappa \end{pmatrix} - \mathring{\boldsymbol{R}}\begin{pmatrix} l \\ \varkappa' \end{pmatrix}\right]}\,. \tag{69}$$

Here M is the proton mass and σ is the number of protons in an elementary cell. As is well known, this system of equations has a solution if, and only if, its determinant vanishes:

$$\det \left| D_{ij}^{\varkappa\varkappa'}(\boldsymbol{q}) - \delta_{ij}\, \delta_{\varkappa\varkappa'}\, M\, \omega^2(\boldsymbol{q}) \right| = 0\,. \tag{70}$$

For every $\boldsymbol{q}$, $\alpha = 3\,\sigma$ the secular equation above possesses solutions $\omega_\alpha(\boldsymbol{q})$ associated with the $3\,\sigma$ polarization vectors which usually are complex. If the contributions to the potential energy of the lattice, given by equations (14) and (48) are substituted into equation (67) one obtains the following expression for the dynamical matrix:

$$D_{ij}^{\varkappa\varkappa'}(\boldsymbol{q}) = E_{ij}^{\varkappa\varkappa'}(\boldsymbol{q}) + C_{ij}^{\varkappa\varkappa'}(\boldsymbol{q}) \tag{71}$$

where

$$E_{ij}^{\varkappa\varkappa'}(\boldsymbol{q}) = \frac{1}{\sigma}\left[\sum_{\boldsymbol{h}} (\boldsymbol{q}+\boldsymbol{h})_i\,(\boldsymbol{q}+\boldsymbol{h})_j\,U_e\,(\boldsymbol{q}+\boldsymbol{h})\,e^{i\boldsymbol{q}\left[\mathring{\boldsymbol{R}}\binom{0}{\varkappa}-\mathring{\boldsymbol{R}}\binom{0}{\varkappa'}\right]}\right.$$
$$\left. - \delta_{\varkappa\varkappa'}\sum_{\boldsymbol{h}\neq 0} (\boldsymbol{h})_i\,(\boldsymbol{h})_j\,U_e(h)\,L(\boldsymbol{h})\right] \tag{72}$$

$$L(\boldsymbol{h}) = \sum_{\varkappa} \cos \boldsymbol{h}\,\mathring{\boldsymbol{R}}\binom{0}{\varkappa}$$

$$U_e(h) = -\frac{V_l^2(Q)}{\varepsilon_e(Q)}\,X(Q) \tag{73}$$

$$C_{ij}^{\varkappa\varkappa'}(\boldsymbol{q}) = M\,\omega_p^2\,C_{ij}'^{\varkappa\varkappa'}(\boldsymbol{q}')\,, \qquad \omega_p^2 = \frac{4\,\pi\,n\,e^2}{M}\,, \qquad q' = q\,r_s \tag{74}$$

$$C_{ij}'^{\varkappa\varkappa'}(\boldsymbol{q}') = -\frac{1}{3}\left\{\sum_{l=0}\frac{1}{\boldsymbol{X}^2\binom{l\,0}{\varkappa\varkappa'}}\left[\left(\frac{3\,X_i\binom{l\,0}{\varkappa\varkappa'}\,X_j\binom{l\,0}{\varkappa\varkappa'}}{\boldsymbol{X}^2\binom{l\,0}{\varkappa\varkappa'}} - \delta_{ij}\right)\left(\frac{G\left[X\binom{l\,0}{\varkappa\varkappa'}\right]}{X\binom{l\,0}{\varkappa\varkappa'}} + \frac{2\,e^{-\boldsymbol{X}^2\binom{l\,0}{\varkappa\varkappa'}}}{\sqrt{\pi}}\right)\right.\right.$$
$$\left.\left. + \frac{4}{\sqrt{\pi}}\,X_i\binom{l\,0}{\varkappa\,\varkappa'}\,X_j\binom{l\,0}{\varkappa\,\varkappa'}\,e^{-\boldsymbol{X}^2\binom{l\,0}{\varkappa\varkappa'}}\right]e^{-i\boldsymbol{q}'\,\boldsymbol{X}\binom{l\,0}{\varkappa\varkappa'}}\right.$$
$$- \delta_{\varkappa\varkappa'}\sum_{l,\varkappa_1}\frac{1}{X^2\binom{l\,0}{\varkappa_1\,0}}\left[\left(\frac{3\,X_i\binom{l\,0}{\varkappa_1\,0}\,X_i\binom{l\,0}{\varkappa_1\,0}}{\boldsymbol{X}^2\binom{l\,0}{\varkappa_1\,0}} - \delta_{ij}\right)\left(\frac{G\left[X\binom{l\,0}{\varkappa_1\,0}\right]}{X\binom{l\,0}{\varkappa_1\,0}} + \frac{2\,e^{-\boldsymbol{X}^2\binom{l\,0}{\varkappa_1\,0}}}{\sqrt{\pi}}\right)\right.$$
$$\left.\left. + \frac{4}{\sqrt{\pi}}\,X_i\binom{l\,0}{\varkappa_1\,0}\,X_j\binom{l\,0}{\varkappa_1\,0}\,e^{-\boldsymbol{X}^2\binom{l\,0}{\varkappa 0}}\right]\right\}$$
$$+ \frac{1}{\sigma}\left[\sum_{\boldsymbol{h}'=0}\frac{(\boldsymbol{h}'+\boldsymbol{q}')_i\,(\boldsymbol{h}'+\boldsymbol{q}')_j}{|\boldsymbol{h}'+\boldsymbol{q}'|^2}\,e^{-(|\boldsymbol{h}'+\boldsymbol{q}'|^2/4)}\,e^{i\boldsymbol{h}'\,\boldsymbol{X}\binom{0\,0}{\varkappa\varkappa'}}\right.$$
$$\left. - \delta_{\varkappa\varkappa'}\sum_{\boldsymbol{h}'\neq 0}\frac{(\boldsymbol{h}')_i\,(\boldsymbol{h}')_j}{(\boldsymbol{h}')^2}\,e^{-(\boldsymbol{h}'^2/4)}\,L(\boldsymbol{h}')\right]$$

ω_P denotes the plasma frequency of protons. It now becomes possible, with the aid of these relations, to calculate the phonon frequencies. To each wave vector $\boldsymbol{q}$ there belong $3\,\sigma$ frequencies. In the neighborhood of the origin in q-space three frequencies will be proportional to $\boldsymbol{q}$. The remaining $3\,(\sigma - 1)$ frequencies will differ from zero at the origin. The dependence $\omega_\alpha = \omega_\alpha(\boldsymbol{q})$ is known as phonon dispersion of branch α ($\alpha = 1, 2, \ldots, 3\,\sigma$). Owing to the translational invariance of the lattice and to the cyclic boundary conditions [28], the entire frequency spectrum is described by $\omega_\alpha = \omega_\alpha(\boldsymbol{q})$ with have vectors $\boldsymbol{q}$ lying within the first Brillouin zone. The quantitaty $\boldsymbol{q}$ takes on N/σ values: N being the total number of protons and σ the number of protons per unit cell.

As an example, Figure 3 illustrates the phonon dispersion in an hcp-lattice with $c/a = 2.03$ and $a = 1.15$ Å, calculated with the help of relations (70), (72) and (73).

Only phonons propagating in directions ΓM and ΓA are considered. The connection between these directions and the first Brillouin zone is shown in Figure 4. The dispersion curves have discontinuities at position indicated by arrows. These so-called KOHN anomalies [29] arise from the singular behavior of the derivatives of $\varepsilon_e(Q)$ and $X(Q)$ at $Q = 2\,k_F$ and have their causes in the sudden change in occupation of electron states on the Fermi sphere. The arrows indicate those values of $\boldsymbol{q}$ for which an anomalous behavior can be expected.

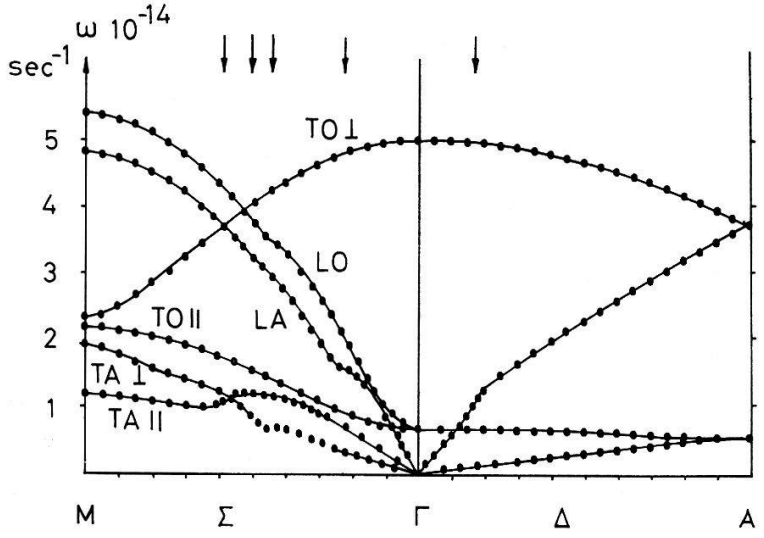

Figure 3

Phonon dispersion curves of metallic hydrogen in the hcp-lattice with $c/a = 2.03$ and $r_s = 0.683$ Å. Arrows indicate $\boldsymbol{q}$ values at which Kohn anomalies can be expected.

In order to be able to analyse the phonon dispersion discussed above it will be necessary to express the frequency in suitable units. If the plasma frequency of ions, ω_P, is chosen as unit, the electrostatic contribution to the dynamical matrix, equation (74), will depend only on crystal structure. Hence, ω_P is the most suitable unit. In order to express electronic and electrostatic contributions to the phonon frequency in these units, consider phonons propagating along ΓA (Fig. 4). In this instance the

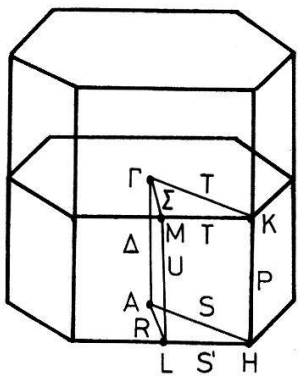

Figure 4

Schematic representation of the first Brillouin zone in a hcp-lattice.

Table II

Solutions of the secular determinant for phonons with wave vector $\boldsymbol{q}$ parallel to ΓA (figure 3). LA = longitudinal acoustic branch, LO = longitudinal optical branch, ΓA = transverse acoustic branch and TO = transverse optical branch.

	Degeneracy	$\omega_p^2\, \Omega^2(\boldsymbol{q}, \alpha)$
LA	1	$D_{33}^{00}(\boldsymbol{q}) + D_{33}^{01}(\boldsymbol{q})$
LO	1	$D_{33}^{00}(\boldsymbol{q}) - D_{33}^{01}(\boldsymbol{q})$
TA	2	$D_{22}^{00}(\boldsymbol{q}) + D_{22}^{01}(\boldsymbol{q})$
TO	2	$D_{22}^{00}(\boldsymbol{q}) - D_{22}^{01}(\boldsymbol{q})$

secular equation can be solved directly. Results are listed in Table II [23]. Using equation (74), the square of these phonon frequencies can be represented in the form

$$\Omega^2(\boldsymbol{q}, \alpha) = \Omega_e^2(\boldsymbol{q}, \alpha) + \Omega_c^2(\boldsymbol{q}, \alpha)\ . \tag{75}$$

In this equation Ω_e^2 and Ω_c^2 refer to the electronic and electrostatic contributions, respectively, to the matrix elements listed in Table II. Table III contains some of the values for Ω^2, Ω_e^2 and Ω_c^2 of the LA- and LO-branches. Corresponding values of single valence hcp-sodium are included for comparison [15]. Ω_c^2 are the frequencies of the proton lattice embedded in a homogeneous sea of negative charge. This lattice is known not to possess any longitudinal acoustic branches (LA). The frequency of these branches as $\boldsymbol{q} \to 0$ tends towards the proton plasma frequency (Table III). The proton induced change in electron density producing a shielding of plasma frequencies is responsible for transforming the longitudinal branches into acoustic ones. This shielding is described by the electronic contributions Ω_e^2. Table III indicates that Ω_e^2 everywhere is greater in metallic hydrogen than in sodium. This difference is mostly due to the electron-proton interaction, to which corresponds the weak pseudo-

Table III

Contributions to the phonon frequency of LA- and LO-branches for $\boldsymbol{q}$ parallel to ΓA (figure 3). H: metallic hydrogen (hcp, $c/a = 2.03$, $r_s = 0.683$ Å). Na: single valence metallic sodium (hcp, $c/a = \sqrt{8/3}$, $r_s = 2.08$ Å).

		H			Na		
	q/q_{max}	Ω_c^2	Ω_e^2	Ω^2	Ω_c^2	Ω_e^2	Ω^2
LA:	0	1	−1	0	1	−1	0
	0.2	0.9993	−0.9872	0.0121	0.9978	−0.9916	0.0062
	0.4	0.9974	−0.9673	0.0300	0.9915	−0.9663	0.0252
	0.6	0.9943	−0.9423	0.0519	0.9815	−0.9252	0.0563
	0.8	0.9904	−0.9121	0.0783	0.9689	−0.8716	0.0973
	1	0.9861	−0.8796	0.1065	0.9549	−0.8100	0.1449
LO:	0	0.9722	−0.7779	0.1942	0.9087	−0.5944	0.3143
	0.2	0.9728	−0.7828	0.1900	0.9110	−0.6077	0.3033
	0.4	0.9748	−0.7926	0.1822	0.9176	−0.6377	0.2799
	0.6	0.9779	−0.8130	0.1649	0.9279	−0.6865	0.2414
	0.8	0.9818	−0.8478	0.1340	0.9407	−0.7463	0.1944
	1	0.9861	−0.8796	0.1065	0.9549	−0.8100	0.1449

potential in sodium. The drastic consequences of this in metallic hydrogen are the exceptionally strong Kohn anomalies (Fig. 3).

In order to estimate the height of these anomalies we shall consider a cubic Bravais lattice. Using equation (72) with $\boldsymbol{q}$ parallel to the [100]-, [110]- or [111]-directions, one obtains the following expression for this lattice, replacing equation (75):

$$\Omega^2(\alpha, \boldsymbol{q}) = \Omega_e^2(\alpha, \boldsymbol{q}) + \Omega_c^2(\alpha, \boldsymbol{q}) \tag{76}$$

where

$$\Omega_e^2(\alpha, \boldsymbol{q}) = \frac{1}{M\,\omega_p^2} \sum_{\boldsymbol{h}\neq 0} [(\boldsymbol{q}+\boldsymbol{h})\,\boldsymbol{e}_\alpha(q)]^2\, U_e\,(\boldsymbol{q}+\boldsymbol{h}) - [\boldsymbol{h}\,\boldsymbol{e}_\alpha(\boldsymbol{q})]^2\, U_e(h) + \frac{1}{M\,\omega_p^2}\,[\boldsymbol{q}\,\boldsymbol{e}_\alpha(\boldsymbol{q})]^2\, U_e(\boldsymbol{q})\,.$$

Hence the height of the Kohn anomalies can be written as

$$2\,\Omega(\alpha, \boldsymbol{q})\,\Delta\Omega(\alpha, \boldsymbol{q}) = -\frac{1}{M\,\omega_p^2}\, S\,\frac{B(2\,k_F)}{6\,\pi}\,(2\,k_F)^2\,(\pm H) = -\frac{1}{2\,k_F\,e^2}\, S(\pm H)\, B(2\,k_F) \tag{77}$$

where

$$Q = 2\,k_F = |\,\boldsymbol{q}+\boldsymbol{h}\,|\,,$$

$$B(2\,k_F) = \frac{18\,\pi\,m}{\hbar^2\,k_F^2}\, V_I^2(2\,k_F)\left[1+\frac{1}{2\,\pi\,a_0\,k_F}\left(1-\frac{1}{4+p}-\frac{1}{p}\right)\right]^{-2} = \frac{2\,e^2}{\pi\,a_0}\left[1+\frac{1}{2\,\pi\,a_0\,k_F}\left(1-\frac{1}{4+p}-\frac{1}{p}\right)\right]^{-2} \tag{78}$$

$$S = \sum_{\boldsymbol{h}}\left[\frac{\boldsymbol{Q}\,\boldsymbol{e}_\alpha(\boldsymbol{Q})}{2\,k_F}\right]^2$$

S is a geometrical factor and H is a constant describing the amount by which $f(Q/2\,k_F)$ deviates from a smooth function. H is positive if $\boldsymbol{q}$ is parallel to $\boldsymbol{h}$ and negative if it is antiparallel. Apart from the purely geometrical factor S, the height of the Kohn anomaly evidently is determined by $B(2\,k_F)$. Furthermore, on referring to equation (78) one recognizes the significance of the bare electron-proton interaction $V_I(Q)$ at $Q = 2\,k_F$. In sodium $V_I(Q)$ corresponds to a weak pseudo-potential having a zero in the neighborhood of $Q = 2\,k_F$ [15]. This difference between sodium and hydrogen is clearly seen in Table IV. A similar difference is shown by the phonon dispersion. While exceptionally strong anomalies appear in metallic hydrogen (Fig. 3) these are barely visible in sodium [15].

Finally, attention is drawn to the connection between height of Kohn anomalies and the behavior of the effective proton-proton interaction. Owing to equations (63) and (64) the potential energy of the lattice can also be written in the form

$$\Phi_0(\mathring{\boldsymbol{R}}) = N\left[\frac{3}{5}\,E_F^0 - \frac{9}{10}\,\frac{e^2}{r_s} - \frac{3\,e^2}{4\,\pi}\,k_F + \varepsilon^{\mathrm{korr}}\right] + \frac{1}{2}\sum_l\sum_{l'}\Phi\,(\mathring{\boldsymbol{R}}^l - \mathring{\boldsymbol{R}}^{l'}) + N\sum_{\boldsymbol{Q}\neq 0} U_e(Q) \tag{79}$$

where

$$\Phi(R) = \frac{1}{(2\,\pi)^3\,n}\int \Phi(Q)\, e^{-i\boldsymbol{Q}\boldsymbol{R}}\, d^3Q\,, \qquad \Phi(Q) = \frac{4\,\pi\,n\,e^2}{Q^2} + U_e(Q)\,. \tag{80}$$

Table IV

Amplitude of Friedel oscillations; H: $r_s = 0.683$ Å.

	H	Na		
$B(2\,k_F)$	25.96	0.03	[15]	10^{-12} erg

Here $\Phi(R)$ is the effective proton-proton interaction. Since the derivative of $U_e(Q)$ has a singularity at $Q = 2\,k_F$, giving rise to the Kohn anomalies in the dispersion of phonons, the behavior of $\Phi(R)$ for large R will be oscillatory. These are the so-called Friedel oscillations which can be considered as a projection mapping of the Fermi surface onto direct space. For large R equations (73) and (80) give

$$\lim_{R\to\infty} \Phi(R) = B(2\,k_F)\,\frac{\cos 2\,k_F\,R}{(2\,k_F\,R)^3}\,.$$

The value $B(2\,k_F)$, equation (78), which determines the height of Kohn anomalies, appears as amplitude of the Friedel oscillations in the equation above. Figure 5 shows the variation of effective proton-proton interaction calculated from relation (80). For comparison, the effective ion-ion interaction in sodium is shown in Figure 6. Oscillations in hydrogen are seen to be very pronounced, in agreement with Table IV, while in sodium they are weak and, in fact, cannot be seen at all in the curve shown.

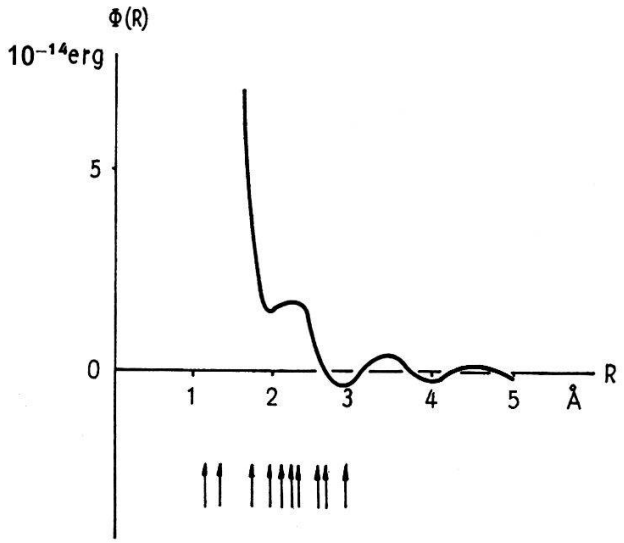

Figure 5

Effective proton-proton interaction for $r_s = 0.683$ Å. Arrows indicate the position of neighbours in the hcp-lattice with $c/a = 2.03$ ($a = 1.15$ Å).

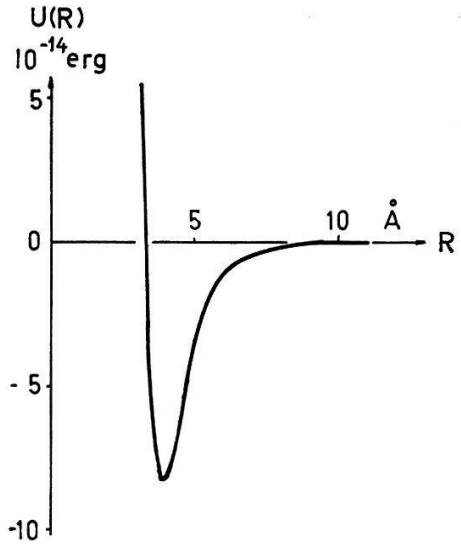

Figure 6

Effective ion-ion interaction in sodium [15].

4. Phase Transition Molecular Crystal-Metal

It is well known that the stable phase possesses the lowest Gibbs energy. At the absolute zero of temperature one has

$$G(P) = E_G - P\,\Omega\,, \qquad P = -\frac{\partial E_G}{\partial \Omega} \tag{81}$$

where E_G is the lattice energy, Ω is the volume and P the pressure. The pressure dependence of the Gibbs energy generally differs for different crystal structures or for different modifications (metal, molecular crystal). Hence, phase transitions can be expected to occur. Two phases α and β are in equilibrium at the point of intersection of the corresponding Gibbs energies $G_\alpha(P)$ and $G_\beta(P)$, i.e.

$$\Delta G(P) = G_\alpha(P) - G_\beta(P) = 0 \,. \tag{82}$$

The pressure defined by this relation is the equilibrium pressure. Following KRONIG et al. [3] we shall consider only molecular and metallic phases.

A discussion of possible transitions from molecular to metallic hydrogen thus requires knowledge of the energies of both phases. The molecular phase will be treated in accordance with the work of TRUBITSYN [7]. The intermolecular interaction will be built up of an intermolecular electron exchange term and a shielded Van der Waals term. Taking account of the zero point energy Trubitsyn derived the following expression for the binding energy per atom:

$$E_B^{mo} = E_G^{mo} - \frac{D}{2} = \Phi^{mo} + E_N^{mo} - \frac{D}{2} \tag{83}$$

where

$$\Phi^{mo} = 1590.7\, e^{-4.838\, n^{-1/3}} - 4.7166\, n^2\,(1 + 1.3076\, n^{2/3})\, e^{-1.0976 n^2}$$

$$E_N^{mo} = 0.01376\, n^{-2/3} \left(\frac{\partial^2 \Phi^{mo}}{\partial (1/n)^2}\right)^{1/2}$$

$$D/2 = 3.6188\, 10^{-12}\ \text{erg} \,.$$

The units are 10^{-12} erg for the coefficients and Å^{-3} for n. The factor $D/2$ is the dissociation energy per atom. This relation now permits calculating the Gibbs energy of the molecular phase. Figure 7 shows the result in the pressure range of interest. To enable us to discuss a possible intersection of this energy curve with that of the metallic phase we require the phonon zero point energy. In principle, this energy can

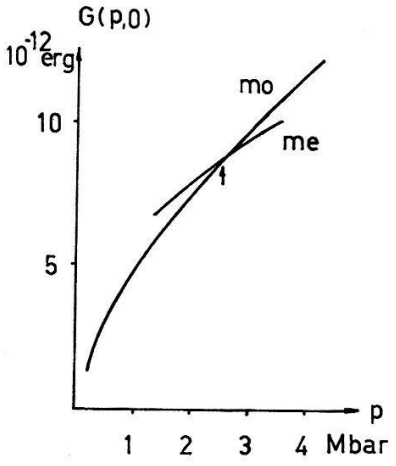

Figure 7

Gibbs energy of molecular and metallic modifications. The following energies are chosen as zeros for $P = 0$: molecular phase: E_G^{mo}, equation (83), metallic phase: $E_G^{me} + D/2 + I$, equation (85). In the metallic phase G was calculated for the crystal structure that is stable at equilibrium, i.e. hcp with $c/a = 2.045$ and $a = 1.15$ Å.

be calculated by use of the secular equation (70) and a method of interpolation developed by GILAT and DOLLING [30]. We shall, however, use an expression given by TRUBITSYN [7] which is independent of crystal structure; i.e.

$$E_N^{me} = \sum_{q,\alpha} \hbar\,\omega_\alpha(q) \approx 1.342\, n^{1/2}\,(1 + 0.01134\, n^{-1/3} - 0.00357\, n^{-2/3}) \tag{84}$$

where the coefficients again are in units of 10^{-12} ergs and n is in units of Å^{-3}. It should be remarked that an explicit calculation of the zero point energies would require extraordinarily long computing times owing to the pronounced Kohn anomalies (Fig. 3). Using equations (61), (65) and (84) results in the expression below for the binding energy of the metallic phase

$$E_B^{me} = E_G^{me} + I = \Phi_0(\Omega) + \Phi_{oe}^s(\mathring{\boldsymbol{R}}) + \Phi_c^s(\mathring{\boldsymbol{R}}) + E_N^{me} + I \tag{85}$$

where I is the ionization energy of a hydrogen atom. The only quantities in this expression which depend on crystal structure are the electronic second order contribution Φ_{oe}^s, equation (65), and the electrostatic term Φ_c^s, equation (65). For any given pressure, the crystal structure with lowest Gibbs energy, equation (81), obviously will be the stable one. Here it should be noted that the zero point energy must be real, or, to put it differently, the microscopic stability condition

$$\omega_\alpha^2(\boldsymbol{Q}) \geqslant 0 \tag{86}$$

must be satisfied. The approximate expression (84), derived by Trubitsyn from the elastic properties, merely assures that

$$\lim_{q\to 0} \omega_\alpha^2(\boldsymbol{q}) \geqslant 0$$

where α comprises the acoustic branches. Under these circumstances the stable crystal structure at any given pressure is that for which the Gibbs energy, equation (85), is a minimum and which satisfies the microscopic condition of stability, equation (86). Bearing this in mind we now use relations (83), (84), (85) and (86) to calculate the Gibbs energy for crystal structures observed in alkali metals. These are the bcc, the fcc and the hcp lattices, where the axis ratio was varied in the interval from 1 to 2.2. Out of these crystal structures the hcp lattice with $c/a = 2.045$ and $a = 1.18$ Å leads to the lowest lying intersection with the Gibbs energy of the molecular phase. Figure 7 shows how the Gibbs energy varies as a function of pressure. In these curves the axis ratio which is stable at the intersection was held fixed. The equilibrium pressure of molecular and metallic phases amounts to 2.60 Mbar. It should be mentioned that the bcc and fcc lattices investigated by CARR [11] are not stable at this pressure. Figures 8 and 9 show the energy and pressure diagrams, respectively. Here again the hcp lattice was assumed for the metallic phase, since it is stable at equilibrium pressure. At this pressure the system changes volume abruptly (Fig. 9). Volumes $V_2 = 2.197$ Å^3 and $V_1 = 1.456$ Å^3 correspond to points having a common tangent in the energy diagram, Figure 9. The physical constants of the metal lattice stable at equilibrium pressure are listed in Table V.

Although the validity of Trubitsyn's model of the molecular phase [7], [10] used here appears to be questionable at the small intermolecular separations resulting at

high pressure, it nevertheless supplies the best quantitative information available at the moment. Considering this uncertainty the data in Table V, particularly those pertaining to equilibrium pressure, must be regarded as merely providing guide lines. In order to estimate the order of magnitude of the uncertainty we have used the expression suggested by KRONIG et al. [3] for the moecular phase. There the pair interaction energy is described by a Lennard-Jones potential, which becomes unrealistic at high pressure [7], [10]. The calculation gave an equilibrium pressure of 1.51 Mbar. Here again, however, the hcp lattice with $c/a = 2.06$, $a = 1.2$ Å and $r_s = 0.715$ Å turned out to be stable. Thus, uncertainties in the description of the molecular phase mainly affect the order of magnitude of the equilibrium pressure.

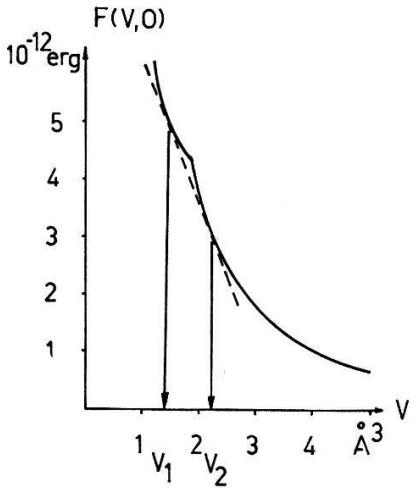

Figure 8

Energy of metallic and molecular phases. The choice of energy zero points corresponds to that of figure 6. The energy difference of points having a common tangent corresponds to the energy increase needed to reduce the volume from V_2 to V_1.

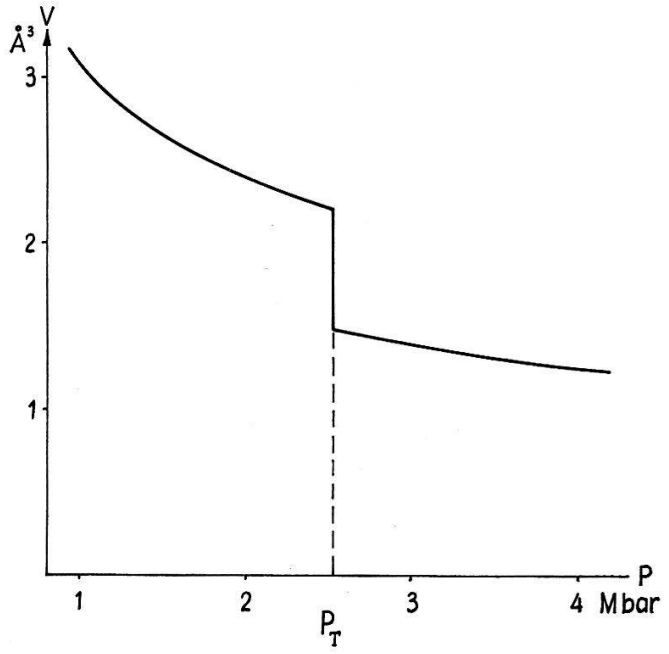

Figure 9

Volume vs. pressure diagram.

Table V

List of physical constants at equilibrium pressure.

Fermi wave number	$k_F = 2.729$ Å^{-1}
Wigner Seitz radius	$r_s = 0.7031$ Å
	$V_1 = 1.456$ Å^3
	$c = 2.197$ Å
	$a = 1.18$ Å
	$c/a = 2.045$
Equilibrium pressure	$P_T = 2.60$ Mbar
	$V_2 = 2.197$ Å^3

It is surprising that among the crystal structures investigated only the tight-packed hexagonal lattice is stable, and that the axis ratio at equilibrium pressure deviates strongly from the ideal value. Since the electrostatic contribution to the lattice energy in bcc-lattices is extremely small (cf. Table I), stability of the hcp-lattice and the deviation if its axis ratio from the ideal value must be due to the electronic contribution Φ^s_{oe}, equation (65). Actually, this deformation decreases with increasing pressure, or with decreasing volume. At a pressure of $P = 117$ Mbar ($r_s = 0.4$ Å) it again is the hcp lattice which is stable, but this time with the ideal axis ration ($c/a = \sqrt{8/3}$). At still smaller volumes the bcc-lattice turns out to be stable. In this connection it should be noted that:

(a) A decreasing radius r_s increasingly favors the bcc-lattice (due to the electrostatic contribution to the lattice energy (equation (65), Table I)).

(b) For the volumes considered here the dielectric function of the electron gas, equation (42), is nearly constant for all reciprocal lattice vectors $\boldsymbol{h}$.

(c) Φ^s_{oe}, equation (65), increases with increasing distortion of the hcp-lattice.

The increase mentioned under (c) is clearly shown in Figure 10. The following explanation can thus be given for the stability of the distorted hcp-lattice at equilibrium pressure, the decreasing distortion with decreasing volume, and the transition to the bcc-lattice: At large r_s, i.e. $r_s \gtrsim 0.7$ Å, the electrostatic contribution is too small to compensate the energy of deformation (c). Φ^s_c, on the other hand, increases with decreasing r_s, while the electronic contribution to the lattice energy, Φ^s_{oe}, remains nearly constant (b). This leads to a compensation of the electronic deformation energy which, at a certain value of r_s (0.4 Å) will lead to a stabilization of the ideal axis ratio. Finally, at still smaller values of r_s a phase transition from the ideal tight-packed hcp-lattice to the bcc-lattice will take place in accordance with (a) and (b).

It may be remarked that the abrupt change of $U_e(Q)$ at $Q = 2\,k_F$, leading to the Kohn effect in phonon dispersion and to Friedel oscillations in the pair interaction energy, hardly influences stability and distortion of the lattice. On the whole, lattice stability is governed by a delicate balance between electronic and electrostatic contributions to the lattice energy, equation (65), where the electrostatic term favors the bcc-lattice.

Next, we should like to point out the connection between electronic contribution to the lattice energy, Φ^s_{oe}, and the density distribution of electrons. This density

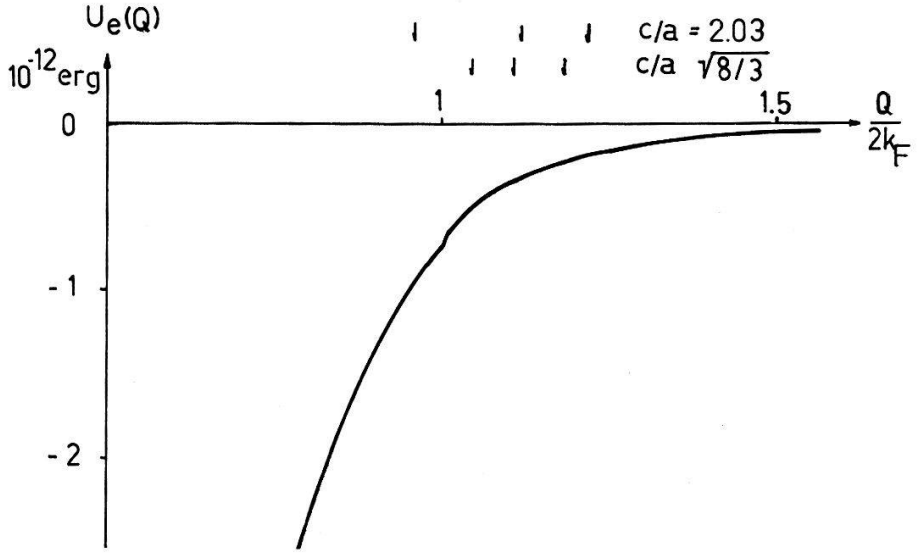

Figure 10

Fourier transform of the electronic contribution to the effective proton-proton interaction for $r_s = 0.683$ Å. Arrows point to the first three neighbouring shells in the reciprocal lattice with $c/a = 2.03$ and $c/a = \sqrt{8/3}$.

distribution can be calculated with the help of equations (25), (31), (38) and (41). The result is given below

$$\varrho(\boldsymbol{r}) = 2 \sum_{\boldsymbol{k} \leqslant k_F} \varphi_{\boldsymbol{k}}^*(\boldsymbol{r})\, \varphi_{\boldsymbol{k}}(\boldsymbol{r}) = n + \varrho^1(\boldsymbol{r}) \tag{87}$$

where

$$\varrho^1(\boldsymbol{r}) = \sum_{l,\varkappa} \varrho_I^1 \left(\boldsymbol{r} - \mathring{\boldsymbol{R}} \binom{l}{\varkappa} \right)$$

$$\varrho_I^1(x) = \frac{1}{N} \sum_{Q \neq 0} e^{i Q X}\, \varrho_I^1(Q) = - \frac{1}{2\pi^2 X} \int_0^\infty U_I(Q)\, X(Q) \sin Q\, X\, Q\, dQ - n\, \Theta\,(r_s - r)$$

$$\varrho_I^1(Q) = -n\, U_I(Q)\, X(Q)\,. \tag{88}$$

In the equation above, n is the density of free electrons and $\varrho^1(r)$ is the first order perturbation arising from the self-consistent electron-proton interaction. Using equations (65) and (88) one obtains the following relation between density distribution $\varrho^1(r)$ and electronic contribution to the lattice energy:

$$\begin{aligned} \Phi_{oe}^s(\mathring{\boldsymbol{R}}) &= \frac{1}{2} \sum_{\boldsymbol{h} \neq 0} |F(\boldsymbol{h})|^2\, U_e(h) = -\frac{1}{2} \sum_{\boldsymbol{h} \neq 0} |F(\boldsymbol{h})|^2\, V_I(h)\, U_I(h)\, X(h) \\ &= \int d^3r\, V_I(r)\, \varrho^1(\boldsymbol{r}) - \int d^3r\, V_I(r)\, \varrho_I^1(r) + \sum_{Q \neq 0} U_e(Q) \\ &= \int d^3r\, V_I(r)\, \varrho^1(\boldsymbol{r}) = -\int d^3r\, \frac{e}{r}\, e\, \varrho^1(\boldsymbol{r})\,. \end{aligned} \tag{89}$$

The structure dependent electronic contribution to the lattice energy thus corresponds to the Coulomb interaction of a proton with the inhomogeneous part of the electron density $\varrho^1(\boldsymbol{r})$, where equation (88) depends on crystal structure. Figures 11 and 12

show the electron density $\varrho(\boldsymbol{r})$ in the (001) and (010) planes, respectively, for $c/a = 2.03$ and $r_s = 0.683$ Å. It is evident that atomic characteristics predominate in the neighborhood of protons, while only small deviations from the mean density take place at intermediate positions. This indicates that electrons are not bound to individual

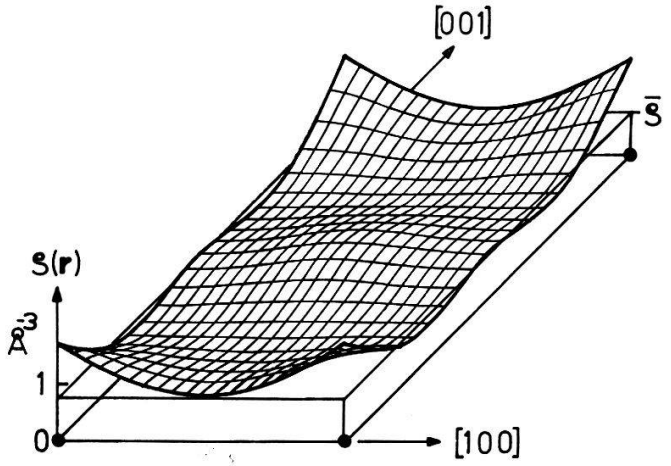

Figure 11

Density distribution of electrons in metallic hydrogen in the (010)-plane for $c/a = 2.03$ and $r_s = 0.683$ Å.

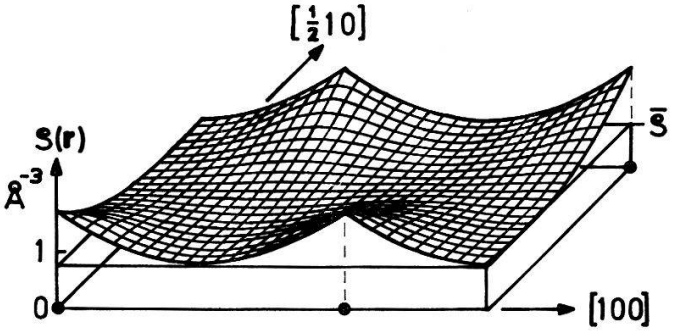

Figure 12

Density distribution of electrons in metallic hydrogen in the (001)-plane for $c/a = 2.03$ and $r_s = 0.683$ Å.

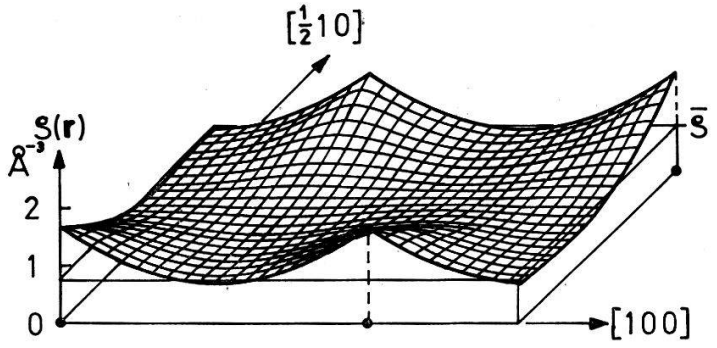

Figure 13

Density distribution of electrons in metallic hydrogen in the (001) plane for $c/a = \sqrt{8/3}$ and $r = 0.4$ Å.

protons or proton pairs but are subject to the combined field of all protons. This behavior is characteristic of metallic binding. For comparison, the electron density in the (001)-plane is shown in Figure 13 for $c/a = \sqrt{8/3}$ and $r_s = 0.4$ Å. Since Φ^s_{oe} is nearly volume independent the difference between density distribution in Figures 12 and 13 must be due to the difference in axis ratios. It should be remembered that these differences lead to the decrease in electronic deformation energy mentioned above.

Table VI lists individual contributions to the lattice energy of the hcp-lattice for $r_s = 0.68$ Å. The first four terms, depending on volume only, evidently contribute the major part to the lattice energy. These terms describe the energy per electron of a Wigner-Seitz sphere filled with free electrons and consist of zero point energy, exchange energy and correlation energy of these electrons, in addition to the Coulomb self-energy of electrons and the Coulomb energy of the electron-proton interaction, combined into a single term. Compared to this the second order electronic contribution, Φ^s_{oe}, which depends on volume and crystal structure, equation (65), is relatively small. Hence, use of perturbation theory for calculating the electron ground state energy appears to be justified. The magnitude of the electrostatic term results from the distortion of the hcp-lattice. For the ideal ratio Φ^s_c amounts to only 0.141 10^{-12} erg. The fact that the phonon zero point energy is comparable to Φ^s_{oe} implies metallic hydrogen being a quantum solid and leads to interesting consequences. We note that Φ^s_{oe} is nearly volume-independent, while the phonon zero point energy is proportional to $r_s^{-3/2}$ (84). Hence, at sufficiently small volumes ($r_s \lesssim 0.4$ Å, $P \gtrsim 117$ Mbar, Table VI) the positive zero point energy exceeds $\Phi^s_{oe} + \Phi^s_c$. This suggests a pressure induced transition from the solid to the liquid state under the influence of the phonon zero point energy [31]. It should be noted that Lindemann's semiphenomenological theory of melting [32] leads to a similar result. These results are quite remarkable in the sense that the pressure induced transition in hydrogen is just reversed with respect to helium.

Table VI

Contributions to the lattice energy of the metallic hcp-lattice in units of 10^{-12} erg. $c/a = 2.03$, $r_s = 0.683$ Å and $c/a = \sqrt{8/3}$, $r_s = 0.4$ Å.

r_s	$3/5\, E_F^0$	$-(3e^2/4\pi)\, k_F$	$\varepsilon^{\text{korr}}/N$	$-9e^2/10 r_s$	Φ^s_e	Φ^s_c	E_N	E_G
0.683	28.930	−15.476	−2.332	−30.402	−2.296	0.389	1.172	−20.015
0.400	84.273	−26.415	−2.695	−51.888	−1.988	0.240	2.608	1.526

At present, it hardly seems possible to produce the equilibrium pressure in the laboratory. The required pressures do exist, however, in the large planets which consist predominantly of hydrogen [8], [9]. Various calculations indicate that Jupiter, in particular, consists mostly of hydrogen (78 volume percent) [9]. Below the atmosphere one assumes the existence of a layer consisting of liquid and solid molecular hydrogen. At a relative radius of 0.8 to 0.7 pressure already corresponds to the equilibrium pressure for the molecular and metallic phases of 2 and 3.4 mbar, respectively. Hydrogen below the partially liquid and partially solid outer layer may thus be expected to be in the metallic state.

5. Electronic Band Structure

Starting from free electrons has enabled us to obtain an approximate solution of the Hartree-Fock equation (16). The electron-proton and electron-electron interactions were treated in self-consistent manner as perturbations, and the single electron energy was calculated to second order. Using equation (53) one obtains for the fixed lattice

$$E_{\boldsymbol{k}} = \frac{\hbar^2}{2\,m}\,k^2 - \frac{3}{10}\,\frac{e^2}{r_s} + \mu + \sum_{\boldsymbol{h}\neq 0} |\,F(\boldsymbol{h})\,|^2\,\frac{U_I^2(h)}{E^0_{\boldsymbol{k}} - E^0_{\boldsymbol{k}+\boldsymbol{h}}} \tag{90}$$

where $\boldsymbol{h}$ is a reciprocal lattice vector. Even though the self-consistent electron-proton interaction is treated as perturbation, the second order contribution can nevertheless become quite large. The form of the energy denominator indicates that this will occur in the neighbourhood of the Bragg planes, i.e. when $\boldsymbol{k} = \boldsymbol{k} + \boldsymbol{h}$. To avoid these divergences one has to use the perturbation theory of degenerate systems. In this perturbation calculation one starts with a linear combination of plane waves

$$|\,\boldsymbol{k}) = \sum_{\boldsymbol{h}} a_{\boldsymbol{k}\,\boldsymbol{h}}\,|\,\boldsymbol{k} + \boldsymbol{h}\rangle \tag{91}$$

and introduces U_I as perturbation. Expansion coefficients $a_{\boldsymbol{k}\,\boldsymbol{h}}$ and eigenvalues $E_{\boldsymbol{k}}$ are obtained in well-known manner from the following system of linear equations:

$$\left[\frac{\hbar^2}{2\,m}\,(\boldsymbol{k}-\boldsymbol{h})^2 - E(\boldsymbol{h},\boldsymbol{k})\right] a_{\boldsymbol{k}\,\boldsymbol{h}} + \sum_{\boldsymbol{h}'} F\,(\boldsymbol{h}-\boldsymbol{h}')\,U_I\,(\boldsymbol{h}-\boldsymbol{h}')\,a_{\boldsymbol{k}\,\boldsymbol{h}'} = 0\,. \tag{92}$$

The energies $E(\boldsymbol{h}, \boldsymbol{k})$ result from the condition that equation (92) can have nontrivial solutions if and only if the determinant of equation (92) vanishes

$$\det\left|\left[\frac{\hbar^2}{2\,m}\,(\boldsymbol{k}-\boldsymbol{h})^2 - E(\boldsymbol{h},\boldsymbol{k})\right]\delta_{\boldsymbol{h}\,\boldsymbol{h}'} + F\,(\boldsymbol{h}-\boldsymbol{h}')\,U_I\,(\boldsymbol{h}-\boldsymbol{h}')\right| = 0\,. \tag{93}$$

Solution of this secular determinant now enables calculating the electronic band structure relative to the energy $-3/10(e^2/r_s) + \mu$. Carrying out a numerical calculation requires a reduction in the rank of the matrix and estimating the error incurred in doing so. A detailed description of this method is contained in Ref. [23].

The so-called Fermi surface, i.e. the energy surface $E(k)$ having Fermi energy is of special physical significance. At the absolute zero of temperature one has:

$$\int_0^{E_F} N(E)\,dE = 1 \tag{94}$$

where

$$N(E) = \frac{2}{(2\,\pi)^3\,n}\int \frac{dS_E}{\operatorname{grad}_{\boldsymbol{k}}\,E(\boldsymbol{k})}\,. \tag{95}$$

Here $N(E)$ is the density of states, i.e. the number of energy levels between E and $E + dE$, dS_E in an element of the surface $E(\boldsymbol{k}) = E$, n is the number of electrons per unit volume, and E_F is the Fermi energy.

Figures 14 and 15 show band structures along ΓA, ΓK, KM and $M\Gamma$ obtained by use of equations (93) and (94) for a hcp-lattice with $r_s = 0.683$ and $c/a = 2.03$.

As expected, splitting-up and energy gaps are very pronounced. The energy gap $\Gamma_3^+\Gamma_4^-$ in particular is so large that the Δ_2-branch cannot reach the Fermi energy. Thus, the Fermi surface is open along $A\Gamma$ and in the ΓMK-plane, respectively, as shown in Figures 16 and 4. This opening is caused by the large axis ratio and the strong electron-proton interaction. The large axis ratio reduces the separation $A\Gamma$. As a result, points Γ_3^+ and Γ_4^-, which coincide in the model of free electrons, are moved into the neighbourhood of the Fermi energy. The strong electron-proton interaction,

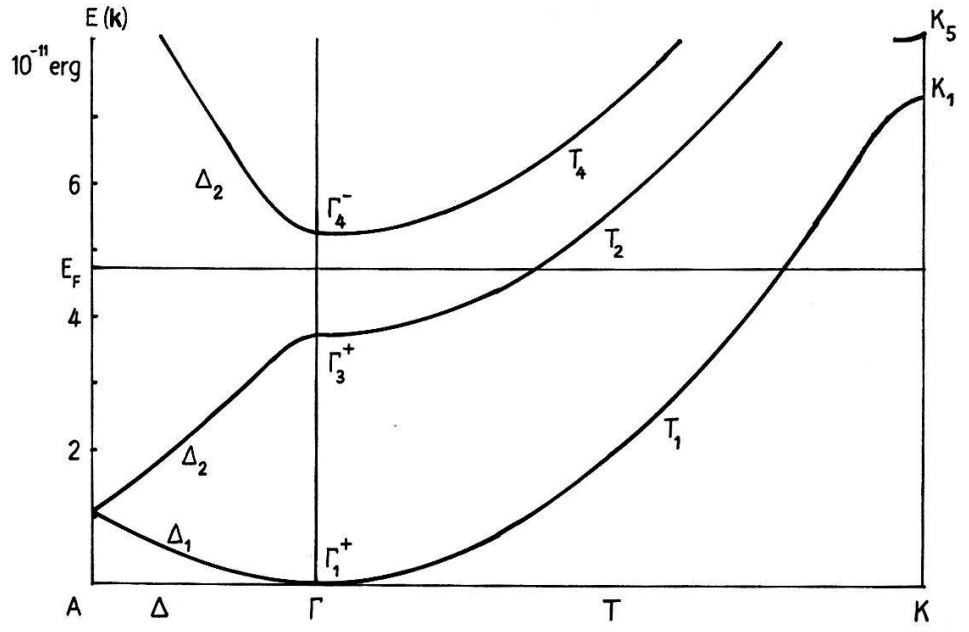

Figure 14

Electronic band structure of metallic hydrogen along Δ and T (figure 4) in units of 10^{-11} erg. E_F denotes Fermi energy. $c/a = 2.03$, $r_s = 0.683$ Å.

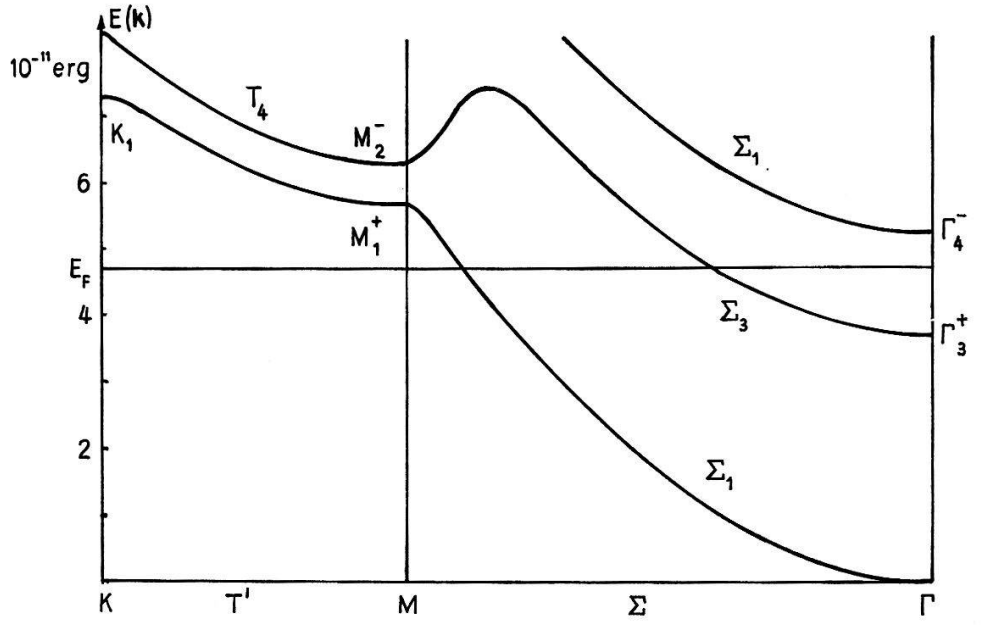

Figure 15

Electronic band structure of metallic hydrogen along T' and Σ (figure 4) in units of 10^{-11} erg. E_F denotes Fermi energy. $c/a = 2.03$, $r_s = 0.683$ Å.

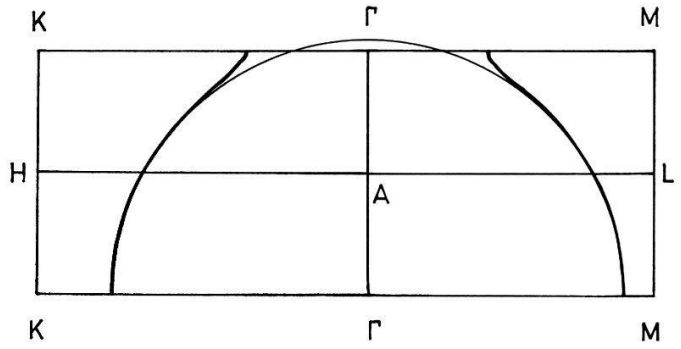

Figure 16

Section through the Fermi surface in extended zone scheme for $c/a = 2.03$ and $r_s = 0.683$ Å.

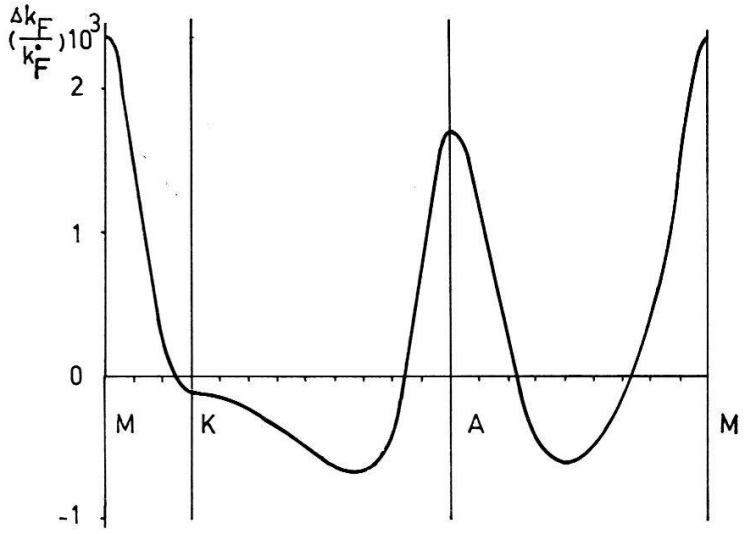

Figure 17

Deviation of Fermi surface from sphericity in metallic hydrogen along the spherical triangle with vertices along ΓM, ΓK and ΓA. $r_s = 0.4$ Å, $c/a = \sqrt{8/3}$.

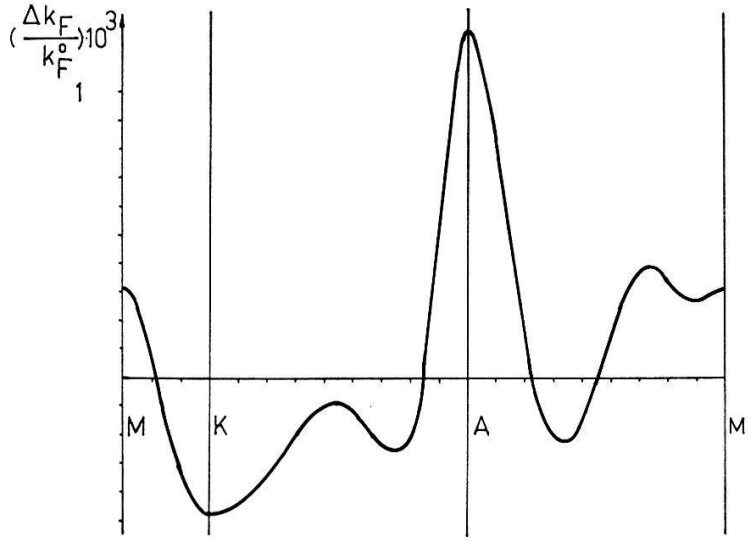

Figure 18

Deviation of the Fermi surface from sphericity in sodium along the spherical triangle with vertices along ΓM, ΓK and ΓA. $c/a = \sqrt{8/3}$.

and the energy gap connected with it, are then sufficient to move Γ_4^- across the Fermi energy and to open up the Fermi surface. Figure 10 shows that a close connection exists between the opening, or the possibility of opening up, and the distortion of the hcp-lattice. Opening up the Fermi surface requires a distortion of the hcp-lattice ($h/2\,k_F \lesssim 1$) leading to an increase in the electronic contribution Φ_{oe}^s, equation (65), to the lattice energy.

As the axis ratio decreases with increasing pressure to become ideal at about 117 Mbar ($r_s = 0.4$ Å) the opening will become smaller and ultimately disappear. The Fermi surface is almost spherical at the ideal axis ratio with $r_s = 0.4$ Å. Figure 17 shows relative deviation from sphericity along a spherical triangle with vertices along ΓA, ΓM and ΓK. Corresponding deviations in hcp-sodium are illustrated in Figure 18 for comparison. Here the pseudopotential model described in [33] was used. Metallic hydrogen, in contrast to sodium, has its greatest deviation in the direction of ΓM. This difference is due to the differences between self-consistent electron-proton interaction and self-consistent pseudo-potential in the neighbourhood of the first reciprocal lattice vectors $\boldsymbol{h}$ (Fig. 19). Deviation ΓM is governed mainly by the value of $U_I(h)$ at the position of the first $\boldsymbol{h}$. In sodium this value is small compared to what it is in metallic hydrogen and smaller than the value at the second nearest $\boldsymbol{h}$. This behavior explains the differences in deviation from sphericity in directions ΓM and ΓA.

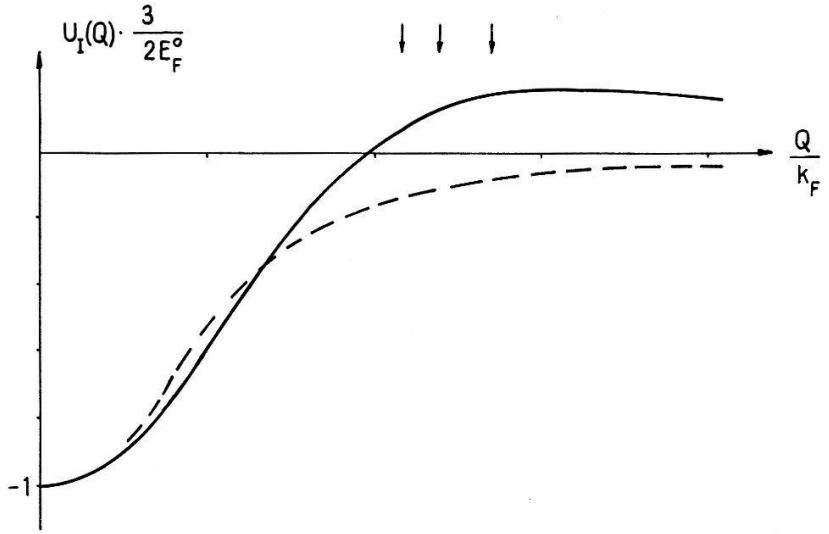

Figure 19

The selfconsistent pseudo-potential of sodium and the self-consistent electron-proton interaction in metallic hydrogen. ——— Na, – – – H. Arrows indicate end points of the first three reciprocal lattice vectors of the hcp-lattice with $c/a = \sqrt{8/3}$.

Besides band structure and Fermi surface there is the change in axis ratio and volume which also influence the density of states, equation (95). The deviation from the free electron model plainly visible in Figure 20 is caused by the energy gap which appears in the band structure (Fig. 14) in Γ and also leads to the opening-up of the Fermi surface. With decreasing volume and axis ratio the energy gap is shifted across the Fermi energy. This fact is clearly shown in Figure 21.

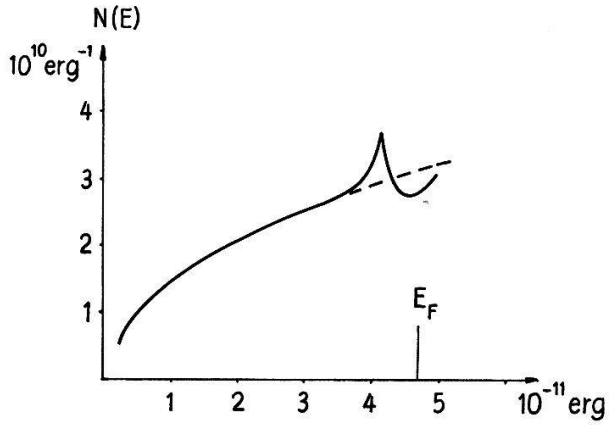

Figure 20

Density of electron states in metallic hydrogen. $c/a = 2.03$, $r_s = 0.683$ Å.
——— effective density of states, – – – density of states for free electrons.

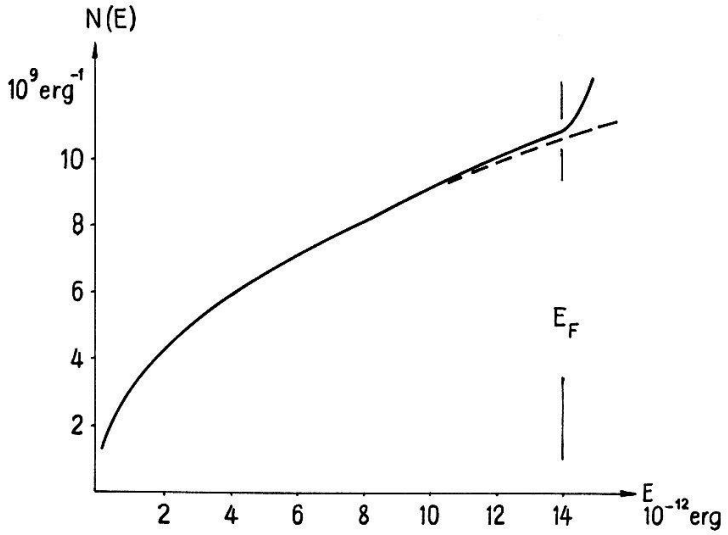

Figure 21

Density of electron states in metallic hydrogen. $c/a = \sqrt{8/3}$, $r_s = 0.4$ Å.
——— effective density of states, – – – density of states for free electrons.

6. Superconductivity

We shall recall briefly some results of the BCS-theory of superconductivity which are essential for the discussion to follow. The basic result of this theory is the formula for the critical temperature [34]

$$k_B T_c = 1.14 \hbar \omega_D e^{-1/g} \approx \hbar \omega_{max} e^{-1/g} \tag{96}$$

where ω_D is the Debye-frequency, ω_{max} is the maximum frequency of phonons, and g is the effective coupling parameter. This coupling parameter is connected both with the contribution of electron-phonon interaction to the density of states λ, and to a term μ^* arising from the electron-electron interaction. Under simplified conditions one finds [35], [39]:

$$g = \frac{\lambda - \mu^*}{1 + \lambda}. \tag{97}$$

Further, we have

$$\mu^* = \frac{\mu}{1+\mu \ln (E_F/\hbar\,\omega_{max})}, \qquad \mu = \frac{1}{2\,\pi\,a_0\,k_F} \ln\,(1 + \pi\,a_0\,k_F)$$

$$\lambda = \frac{m}{4\,\pi^2\,M\,\hbar^2\,k_F\,n} \sum_{\alpha} \int_0^{2k_F} H_\alpha(Q)\; U_I^2(Q)\; Q\; dQ$$

$$H_\alpha(Q) = \frac{1}{4\,\pi} \int d\Omega\; \frac{[\boldsymbol{Q}\; \boldsymbol{e}_\alpha(\boldsymbol{Q})]^2}{\omega_\alpha^2(\boldsymbol{Q})}. \tag{98}$$

Here we assumed a spherical Fermi surface.

In order to evaluate λ we have represented the six phonon branches by three spherical symmetric dispersion curves in the extended zone; one of these is taken to be a purely longitudinal mode and the other two are taken to be degenerate and purely transverse. The extended zone was replaced by an equivalent sphere. The phonon frequencies of the three branches were chosen to be the average over the different q-directions. The final results are given in Table VII. In these calculations the band-structure effects have been neglected. However, it is quite unlikely that this approximation vitiate our estimates. In any case the values of T_c are remarkable. Therefore it may be surmised that metallic hydrogen is a high-temperature superconductor as postulated by ASHCROFT [38]. Furthermore, we can state on the basis of the contents of Table VII that T_c decreases with increasing pressure. This possibility has already been suggested by ABRIKOSOV [37].

In order to understand why T_c decreases under further pressure, it is instructive to look at the parameter λ (98). There is a strong cancellation between the electrostatic and electronic contributions to the phonon frequencies (Table III). Thus the important dependence of λ upon the screened electron proton interaction $U_I(Q)$ arises from $\omega_\alpha^2(Q)$ in the denominator of equation (98), rather than from $U_I^2(Q)$ in the numerator. This is illustrated in Table VII, where λ decreases with increasing ω_D, which leads to a decrease of T_c under further pressure.

From these results one can draw three important conclusions. First, it may be surmised that metallic hydrogen is a high-temperature superconductor. Second, this suggests that if indeed the bulk of Jupiter is composed of hydrogen, part of it may be in the metallic superconducting state, and the association of magnetic fields with permanent currents may be of some significance. Third, under sufficiently high pressure metallic hydrogen may be a superconducting quantum fluid (Table VI, VII).

In a second paper devoted to metallic hydrogen [36] we shall present a more detailed discussion of the high-temperature superconductivity and its pressure dependence in connection with other properties.

Table VII

Parameters of the superconducting state.

r_s	ω_{max}	λ	μ^*	$1/g$	T_c
0.683	3694	0.739	0.101	2.726	242
0.400	9762	0.378	0.083	4.685	90
Å	°K				°K

7. Concluding Remarks

Up untill now there was uncertainty concerning the crystal structure, lattice dynamics, and electronic structure of metallic hydrogen. The present paper is a first attempt to close this gap. In doing so we have used a number of simplifying approximations: the adiabatic and harmonic approximations; a modified Hartree-Fock method for calculating both the ground state energy of electrons and the single-electron properties; a self-consistent solution of the Hartree-Fock equations; an approximate solution of the determining equations for the self-consistent electron-proton interaction, and a local treatment of electron exchange. Regarding the quality of these simplifying approximations one can state that their use has enabled an explanation of numerous properties of simple metals [14], [15], [20]–[24]. In spite of this, we consider it necessary to clarify the quality of the adiabatic approximation and to obtain a numerical solution of the determining equations for the electron-proton potential. A discussion of the problems connected with the adiabatic approximation is contained in a paper by CHESTER [17]. It may be concluded from all this that the investigation presented here gives a true, quantitative picture of metallic hydrogen, except at very small volumes.

It turns out that the electron-proton interaction, which is strong compared with the pseudo-potential of simple metals, leads to remarkable effects. Some of these are: Pronounced Kohn anomalies and Friedel oscillations, high-temperatures superconductivity, and distortion of the hcp-lattice enabling an opening-up of the Fermi surface. An interesting conclusion was the decrease of this distortion with increasing pressure and the pressure-induced transition from the solid to the liquid state under the influence of the phonon zero point energy. It thus seems probable that metallic hydrogen is a superconducting quantum liquid for $r_s \lesssim 0.4$ Å.

Acknowledgements

I should like to express my sincere thanks to Prof. A. A. ABRIKOSOV, Prof. W. BALTENSPERGER, Dr. E. STOLL, Dr. W. B. WAEBER and N. SZABO for helpful suggestions and valuable discussions. I am indebted to Dr. E. STOLL and to the computing centers of ETH and EIR for having carried out the numerical calculations.

References

[1] C. S. BARRETT, L. MEYER and J. WASSERMAN, J. Chem. Phys. *45*, 834 (1966).
[2] E. WIGNER and H. B. HUNTINGTON, J. Chem. Phys. *3*, 764 (1935).
[3] R. KRONIG, J. DE BOER and J. KORRINGA, Physica *12*, 245 (1946).
[4] B. J. DAVYDOV, Trudy Geofiz. Inst. Akad. Nauk. SSSR *26*, 86 (1953).
[5] A. A. ABRIKOSOV, Astr. Zhur. *31*, 112 (1954).
[6] J. C. RAICH, J. Chem. Phys. *45*, 2673 (1966).
[7] V. P. TRUBITSYN, Soviet Solid State *8*, 688 (1966).
[8] W. C. DE MARCUS, Astron. J. *63*, 2 (1958).
[9] *Handbook of the Physical Properties of the Planet Jupiter* (NASA, Washington 1967, NASA Sp-3031).
[10] V. P. TRUBITSYN, Soviet Solid State *7*, 2708 (1966).
[11] W. J. CARR, Phys. Rev. *128*, 120 (1962).
[12] J. L. CALAIS, Arkiv för Fysik *29*, 255 (1965).

[13] N. H. MARCH, Physica *22*, 331 (1965).
[14] W. A. HARRISON, *Pseudopotentials in the Theory of Metals* (Benjamin Inc., New York 1966).
[15] T. SCHNEIDER and E. STOLL, *Neutron Inelastic Scattering* (International Atomic Energy Agency, Wien 1968, Vol. I, p. 101).
[16] M. BORN, Nachr. Akad. Wiss. Göttingen, Nr. 6 (1951).
[17] G. V. CHESTER, Ad. in Phys. *10*, 357 (1961).
[18] K. FUCHS, Proc. Roy. Soc. *A 151*, 585 (1935).
[19] L. KLEINMANN, Phys. Rev. *160*, 585 (1967).
[20] A. O. E. ANIMALU, Phys. Rev. *161*, 445 (1967).
[21] T. SCHNEIDER and E. STOLL, Phys. Lett. *24A*, 258 (1967).
[22] J. E. INGLESFIELD, J. Phys. C. *1*, 1337 (1968).
[23] E. STOLL and T. SCHNEIDER, Phys. Kondens. Mat. *8*, 58 (1968).
[24] D. WEAIRE, J. Phys. C. *1*, 210 (1968).
[25] D. PINES and P. NOZIÈRES, *The Theory of Quantum Liquids* (Benjamin Inc., New York 1966).
[26] D. J. W. GELDART and S. H. VOSKO, Can. J. of Phys. *44*, 2137 (1966).
[27] P. NOZIÈRES and D. PINES, Nuovo Cim. *9*, 470 (1958).
[28] A. A. MARADUDIN, E. W. MONTROLL and G. H. WEISS, *The Theory of Lattice Dynamics in the Harmonic Approximation* (Academic Press, New York 1963).
[29] W. KOHN, Phys. Rev. Lett. *2*, 393 (1959).
[30] G. GILAT and G. DOLLING, Phys. Rev. Lett. *8*, 304 (1964).
[31] A. A. ABRIKOSOV, Soviet Phys. JETP *12*, 1254 (1961).
[32] D. PINES, *Elementary Excitations in Solids* (Benjamin Inc., New York 1966), p. 34.
[33] T. SCHNEIDER and E. STOLL, Phys. kondens. Mat. *6*, 135 (1967).
[34] J. F. SCHRIEFFER, *Theory of Superconductivity* (Benjamin Inc., New York 1966), p. 188.
[35] T. SCHNEIDER, E. STOLL and W. BÜHRER, Helv. phys. Acta *42*, 46 (1969).
[36] T. SCHNEIDER and E. STOLL, to be published.
[37] A. A. ABRIKOSOV, Soviet Phys. JETP *14*, 408 (1962).
[38] N. W. ASHCROFT, Phys. Rev. Lett. *21*, 1748 (1968).
[39] W. L. MCMILLAN, Phys. Rev. *167*, 331 (1968).